Combined Inhibition of DYRK1A, SMAD and Trithorax Pathways Synergizes to Induce Robust Replication in Adult Human Beta Cells

Peng Wang, PhD[#1], Esra Karakose, PhD[#1], Hongtao Liu, BS[1], Ethan Swartz, BS[1], Courtney Ackeifi, BS[1], Viktor Zlatanic, BS[1], Jessica Wilson, BS[1], Bryan J. González, MPhil[3], Aaron Bender, BS[1], Karen K. Takane, PhD[1], Lillian Ye, BS[4], George Harb, PhD[4], Felicia Pagliuca, PhD[4], Dirk Homann, MD[1], Dieter Egli, PhD[3], Carmen Argmann, PhD[3], Donald K. Scott, PhD[1], Adolfo Garcia-Ocaña, PhD[1], and Andrew F. Stewart, MD[1,5]

[1]Diabetes Obesity and Metabolism Institute, New York, NY 10029

[2]The Department of Genetics and Genomic Sciences, The Icahn Institute for Genomics and Multiscale Biology, The Icahn School of Medicine at Mount Sinai, New York, NY 10029

[3]The Naomi Berrie Diabetes Center, Columbia University, New York, NY 10032

[4]Semma Therapeutics, Cambridge, MA 02142

[5]Lead contact

[#] These authors contributed equally to this work.

Summary

Small molecule inhibitors of dual specificity tyrosine-regulated kinase 1A (DYRK1A) induce human beta cells to proliferate, generating a labeling index of 1.5-3%. Here, we demonstrate that combined pharmacologic inhibition of DYRK1A and transforming growth factor beta superfamily (TGFβSF)/SMAD signaling generates remarkable further synergistic increases in human beta cell proliferation (average labeling index, 5-8%, and as high as 15-18%), and increases in both mouse and human beta cell numbers. This synergy reflects activation of cyclins and cdks by DYRK1A inhibition, accompanied by simultaneous reductions in key cell cycle inhibitors (*CDKN1C, CDKN1A*). The latter results from interference with the basal Trithorax- and SMAD-mediated transactivation of *CDKN1C* and *CDKN1A*. Notably, combined DYRK1A and TGFβ inhibition

allows preservation of beta cell differentiated function. These beneficial effects extend from normal human beta cells and stem cell-derived human beta cells to those from people with Type 2 diabetes, and occur both *in vitro* and *in vivo*.

Graphical Abstract
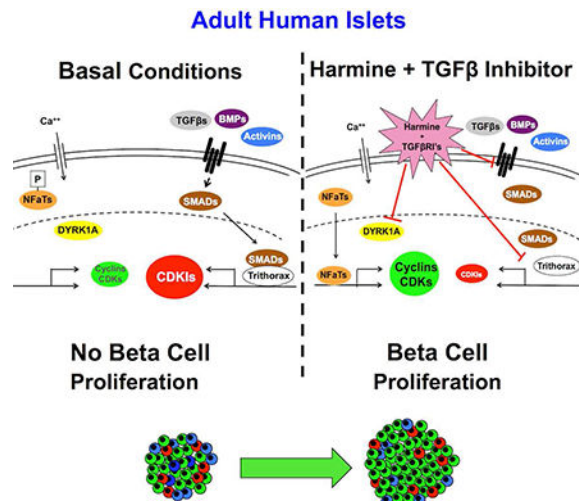
eTOC Blurb:

Adult human pancreatic beta cells are notoriously resistant to replication. XXX et al find that the combination of the DYRK1A inhibitor, harmine, with an inhibitor of the TGFβ superfamily of receptors induces synergistic increases in human beta cell cells in vitro and in vivo through enhanced differentiation.

Introduction

Inhibition of the enzyme dual-specificity tyrosine phosphorylation-regulated kinase 1A (DYRK1A) in human beta cells, using drugs such as harmine, INDY, GNF4877, 5-iodotubericidin (5-IT) or CC-401, is able to induce proliferation (labeling indices) in the 1.5-3% range, as assessed using Ki67, EdU, BrdU and/or PCNA immunolabeling of insulin-containing cells derived from human cadaveric islets (Aamodt et al., 2016; Abdolazimi et al., 2018; Dirice et al., 2016; Shen et al., 2015; Wang et al., 2015a; Wang et al., 2016). This notable accomplishment, confirmed in multiple laboratories, replicates the proliferation "rate" in human beta cells in the first year of life, the only stage of human development at which appreciable beta cell proliferation occurs (Gregg et al., 2012; Kassem et al., 2000; Meier et al., 2008; Wang et al., 2015b). One can reasonably assume that more rapid beta cell proliferation would be attractive in order to replete or restore beta cell mass to normal in people with Type 1 and Type 2 diabetes. Since complete silencing of DYRK1A in human beta cells does not appreciably further increase proliferation (Dirice et al., 2016; Wang et al., 2015a), we surmised that combination treatment with other classes of potential beta cell mitogenic small molecules might enhance efficacy of harmine analogues. We selected TGFβSF receptor inhibitors for combination therapy for several reasons. First, in genomic

and transcriptomic analyses of beta cell mitogenic pathways in human insulinoma, SMAD signaling and chromatin remodeling pathways were the most statistically significant (Wang et al., 2017). Second, as described below, we observed that TGFβSF members were abundant in isolated human beta cells, and some were affected by pharmacologic DYRK1A inhibition. Third, Gittes et al, Kim et al, Bhushan, Kulkarni et al, Schneyer et al, Teramoto et al and Annes et al (Abdolazimi et al., 2018; Brown and Schneyer, 2010; Brown et al., 2014; Dhawan et al., 2016; El-Gohary et al., 2014; Mukherjee et al., 2007; Nomura et al., 2014; Smart et al., 2006; Xiao et al., 2016; Xiao et al., 2014; Zhou et al., 2013) have each reported that genetic or pharmacologic TGFβSF pathway inhibition in rodent beta cells can lead to rodent beta cell proliferation.

Transforming growth factor beta superfamily (TGFβSF) signaling is complex (Antebi et al., 2017; Brown and Schneyer, 2010; Brown et al., 2014; Dhawan et al., 2016; El-Gohary et al., 2014; Gaarenstroom and Hill, 2014; Macias et al., 2015; Mukherjee et al., 2007; Nomura et al., 2014; Smart et al., 2006; Stewart et al., 2015; Xiao et al., 2016; Xiao et al., 2014; Zhou et al., 2013). In its simplest form, it involves a series of ligands (e.g., TGFβ's 1,2,3, activins, inhibins, glia-derived factors, bone morphogenic proteins), a series of cognate receptors, a repertoire of endogenous inhibitors (e.g., sclerostin, follistatin-like factors), that signal downstream through a series of activating or receptor R-SMADs (SMADs 1,2,3,5,8/9), and the co-SMAD, SMAD4, and are blocked by one of two inhibitory I-SMADs (SMADs 6,7). Once activated, R-SMAD heteromers translocate to the nucleus where they serve individually or in complexes to transactivate or repress target genes. Notably, at some of these loci, SMADs integrate into epigenetic chromatin-modifying complexes, such as the trithorax group complex (TrxG) that includes histone methylases (e.g., MEN1) and histone demethlyases (e.g., KDM6A) that regulate chromatin access (Antebi et al., 2017; Brown and Schneyer, 2010; Brown et al., 2014; Dhawan et al., 2016; El-Gohary et al., 2014; Gaarenstroom and Hill, 2014; Macias et al., 2015; Mukherjee et al., 2007; Nomura et al., 2014; Smart et al., 2006; Stewart et al., 2015; Xiao et al., 2016; Xiao et al., 2014; Zhou et al., 2013).

In this report, we demonstrate that combined pharmacologic or genetic inhibition of DYRK1A and TGFβSF signaling induces remarkable and previously unattainable rates of human beta cell proliferation *in vitro* and *in vivo*, and actually increases human and mouse beta cell numbers. We explore the underlying mechanisms that drive this remarkable rate of proliferation, and show that the results apply not only to beta cells from normal cadaveric human islets, but also to human stem cell (hESC)-derived beta cells, and those from people with Type 2 diabetes.

Results

Combinations of DYRK1A inhibitors and TGFβSF Inhibitors Induce Synergistic Human Beta Cell Proliferation and Increase Beta Cell Numbers.

Gene expression profiles from FACS-sorted human beta cells (Wang et al., 2017) were remarkable for the abundance of select members of the TGFβSF. In addition, harmine treatment of human islets resulted in notable changes in TGFβSF members (**Supplemental Tables** 1 and 2). Reasoning from these observations, from the prominence of SMAD

signaling in human insulinoma cell proliferation (Wang et al., 2017), and the beneficial effects of TGFβ signaling inhibition in mouse islets described by Bhushan, Gittes, Kim, Schneyer, Teramoto et al (Brown and Schneyer, 2010; Brown et al., 2014; Dhawan et al., 2016; El-Gohary et al., 2014; Mukherjee et al., 2007; Nomura et al., 2014; Smart et al., 2006; Xiao et al., 2016; Xiao et al., 2014; Zhou et al., 2013), we explored the effects of TGFβSF pharmacologic inhibitors on human beta cell proliferation in a large number of human cadaveric islet preparations (Figure 1A-C). Vehicle alone (DMSO) had no effect, and harmine displayed its usual ~2% labeling index (Wang et al., 2015a), as assessed using Ki67 labeling of insulin-positive cells. A broad range of TGFβ receptor, BMP receptor and activin receptor inhibitors had little effect on human beta cell proliferation, as previously reported (Dhawan et al., 2016). In contrast, every TGFβSF receptor inhibitor tested, whether targeting TGFβ, activin or BMP receptors, when used in combination with harmine, induced dramatic increases in the Ki67 labeling index in human beta cells. Proliferation rates (labeling indices) averaged in the 5-8% range; the large error bars reflect even higher proliferation rates in occasional human islet preparations, sometimes achieving Ki67 labeling indices as high as 15-18%. These results were independently confirmed using automated, high throughput, high content imaging of human HUES8 hESC-derived beta cells (Supplemental Figure 1) (Pagliuca et al., 2014).

The beneficial effects were not confined to harmine, but extended to additional DYRK1A inhibitors, including INDY and leucettine-41 (Tahtouh et al., 2012) (Figure 1D,E). In addition, in dose-response studies, the combinations fulfilled formal criteria for pharmacologic synergy (Supplemental Figure 2A,B). Further, the remarkable synergy could be observed with two additional measures of proliferation BrdU incorporation and phospho-histone-H3 immunolabeling (Figure 1F,G, Supplemental Figure 2C,D).

Notably, the mitogenic effects of the combination were not specific to beta cells: frequent proliferation was observed in alpha, delta, PP, ductal and other non-beta cells within the islet as well (Figure 1B, red arrows, Supplemental Figure 3AB). No adverse effects were observed with respect to beta cell death or DNA damage, as assessed by TUNEL assay and γH2AX immunolabeling, respectively (Supplemental Figure 3C-E).

We next examined whether harmine together with the TGFβ inhibitor, LY364947, could increase actual numbers of human beta cells, using two different approaches. First, using adult human cadaveric islets, we employed flow cytometry to count the numbers of live human beta cells, previously labeled with an insulin promoter-driven adenovirus expressing the bright green fluorescent protein, ZsGreen (Wang et al., 2017), following four days of exposure to vehicle or the harmine-LY364947 combination. As illustrated in Figure 1H, absolute beta cell numbers increased in six of seven human islet preparations treated with the harmine-LY364947 combination, as compared to the same human islets treated with vehicle. Second, to confirm these results independently, we used Mel1 hESC expressing GFP in one allele of the insulin locus (Micallef et al., 2012), differentiated into beta cells (Sui et al., 2018). Figure 1I illustrates the dramatic increase in absolute GFP[+] cell numbers in these hESC-derived cultures. Together, these findings demonstrate that the harmine-LY364947 combination can increase not only markers of beta cell proliferation, but actual numbers of both stem cell-derived as well as adult human beta cells.

Harmine-TGFβSF Combinations Enhance Markers of Human Beta Cell Differentiation in Normal and Type 2 Diabetes Islets.

Concerned that activation of mitogenic pathways might lead to de-differentiation of beta cells, we explored gene expression of a panel of markers of beta cell differentiation (Figure 2AB). As we had observed for harmine alone (Wang et al., 2015a), the harmine-TGFβSF inhibitor combination not only failed to induce de-differentiation, the opposite occurred: gene expression of key beta cell markers such as *PDX1, NKX6.1, MAFA, MAFB, SLC2A2*, and *PCSK1* all increased with combined harmine-TGFβSF inhibitor treatment, as assessed on whole islets by qPCR; *ISL1, SLC2A1, NEUROD, NKX2.2, PCSK2* all remained the same as at baseline. Only *PAX4* declined, the significance of which is uncertain. These results were confirmed and expanded using massively parallel RNA sequencing of human cadaveric islets treated with the harmine-TGFβSF inhibitor combination (**Supplemental Tables** 1,2). Immunocytochemistry in dispersed human islet preparations confirmed the increases in PDX1, NKX6.1 and MAFA specifically in human beta cells (Figure 2C, Supplemental Figure 4A). Further, RNA sequencing demonstrated that so-called "disallowed" or "forbidden" beta cell genes (Pullen and Rutter, 2013; Schuit et al., 2012) were not altered by the harmine-TGFβSF inhibitor combination (Supplemental Table 2). In line with the observations above, glucose-stimulated insulin secretion was normal, and possibly accentuated, in human islets treated with the harmine-TGFβSF inhibitor combination (Figure 2D).

Since de-differentiation of beta cells occurs in both mice and humans with Type 2 diabetes (Cinti et al., 2016; Talchai et al., 2012), we next explored proliferation in islets derived from six donors with Type 2 diabetes (Figure 2E). Remarkably, harmine alone increased Ki67 immunolabeling to the same degree observed in non-diabetic islet donors (Wang et al., 2015a). Moreover, harmine in combination with three different TGFβSF inhibitors (LY364947, ALK5, GW788388) led to synergistic increases in Ki67 labeling, as had been observed in normal islets (**Figures** 1,2). Equally remarkably, harmine in combination with the TGFβSF inhibitor, ALK5, also led to significant increases in expression of *PDX1, NKX6.1* and *MAFA* in human T2D islets (Figure 2F), results that extend to the combination of harmine plus GW788388 or LY364947 (Supplemental Figure 4B).

Combined Harmine-TGFβSF Inhibition Efficacy Requires SMAD and DYRK1A Signaling.

TGFβSF ligands affect SMAD signaling but may also recruit other signaling pathways (Antebi et al., 2017; Brown and Schneyer, 2010; Stewart et al., 2015). To ascertain whether the harmine-TGFβSF inhibitor combination affected SMAD signaling, human islets were incubated with harmine alone or in combination with two TGFβSF inhibitors, LY364947 or ALK5 and the expression levels of various SMADs was assessed (Figure 3A). The harmine-TGFβSF inhibitor combinations led to reductions in SMAD3 phosphorylation without altering SMAD2/3 abundance, and also led to dramatic reductions in total SMADs 1/5/9 (note that antisera do not distinguish between these three SMADs). Perhaps most interestingly, harmine alone led to reductions in phospho-SMAD3 as well as to reductions in total SMAD1/5/9, a result that extends the apparent reduced expression of select TGFβSF members noted earlier in Supplemental Table 2.

To explore the requirement for SMAD signaling in the proliferation induced by the harmine-TGFβSF inhibitor combinations, we used adenoviruses expressing shRNAs directed against the R-SMADs 2 and 3 and their co-SMAD, SMAD4, in human islets treated with harmine (Figure 3B). We observed that silencing these three R-SMADs further enhanced harmine-induced human beta cell proliferation. Conversely, overexpressing the I-SMADs 6 and 7 by themselves had no effect on proliferation, but markedly enhanced harmine-induced proliferation (Figure 3CD). Collectively these results reveal three key insights. First, the proliferation generated by the TGFβSF inhibitors when given in combination with harmine is mediated in large part or entirely via SMAD signaling, since silencing R-SMADs or overexpressing I-SMADs was able to substitute for TGFβSF inhibitors in the combination. Second, harmine itself has previously unrecognized inhibitory effects on SMAD signaling at the protein level (SMADs1/5/9 and phospho-SMAD3). And third, multiple SMAD families (i.e., both the canonical TGFβ receptor-associated SMADs 2,3 and 4 as well as the canonical BMP receptor-associated SMADs 1,5,8/9) participate in harmine-mediated proliferation.

Harmine analogues derive their mitogenic effects in large part, if not exclusively, via inhibition of DYRK1A (Abdolazimi et al., 2018; Dirice et al., 2016; Shen et al., 2015; Wang et al., 2015a). To explore the presumed requirement for DYRK1A in the synergistic proliferation derived from the harmine-TGFβ inhibitor combination, we employed adenoviral silencing and overexpression of DYRK1A, alone or in combination with TGFβSF inhibition (Figure 3E-G). These experiments reveal that DYRK1A silencing/loss markedly accentuates proliferation induced by the TGFβ inhibitors GW788388 and LY364947, and conversely that DYRK1A overexpression is able to block proliferative effects of the harmine-TGFβ inhibitor combination. Collectively, the studies in Figure 3 illustrate that the majority, if not all, of the synergistic effects of the harmine-TGFβ inhibitor combination on human beta cell proliferation are attributable to combined interruption of both DYRK1A and SMAD signaling. They further reveal that harmine can have unanticipated direct or indirect effects on SMADs to reduce TGFβSF signaling.

The Harmine-TGFβSF Inhibitor Synergy Reflects Complementary Effects on Cyclins/CDKs and CDK Inhibitors.

Reasoning that harmine and harmine-TGFβSF inhibitors (and DYRK1A and SMADs, respectively) must ultimately orchestrate cell cycle entry via cell cycle activators and cell cycle inhibitors, we examined gene expression of cell cycle activators and inhibitors in whole islets treated with vehicle, harmine, TGFβ inhibitor or the harmine-TGFβ inhibitor combination (Figure 4AB). Harmine alone, as described previously (Wang et al., 2015a), induced expression of a number of cell cycle activators (e.g., *CDK1, CCNA1, CCNE2* and *CDC25A*). In contrast, TGFβ inhibition alone had little effect on cell cycle activators. Notably, the harmine-TGFβ inhibitor combination induced no further activation of these or other cyclins or cdks: the harmine-TGFβ inhibitor combination was similar to harmine alone. These results were independently confirmed and extended by RNAseq of human islets (**Supplemental Tables** 1,2).

Cell cycle inhibitors behaved differently (Figure 4B). Harmine alone had modest and limited effects on cell cycle inhibitor expression, with the exception of *CDKN1C* (encoding

p57^{KIP2}) which declined by ~50% as described previously (Wang et al., 2015a). In contrast, TGFβ inhibition alone, or in combination with harmine, reduced expression of *CDKN2B* (encoding p15^{INK4b}), *CDKN1A* (encoding p21^{CIP}) and *CDKN1C*/p57^{KIP2}. There was also a small but significant reduction in *CDKN2A* (encoding p16^{INK4a}). There was no change in the expression of *CDKN1B* (encoding p27^{CIP}), an important inhibitor of cell cycle progression the mouse beta cell. These results also were independently confirmed and extended by RNAseq of human islets (**Supplemental Tables** 1,2).

To explore the mechanism underlying the decline in *CDKN1A, CDKN1C* and *CDKN2B* in response to TGFβ inhibition, we used adenoviruses to silence R-SMADs 2,3 and 4, or to overexpress I-SMADs 6 and 7 in human islets, and queried effects on *CDKN1A, CDKN1C* and *CDKN2B* expression. Silencing the R-SMADs or overexpressing I-SMADs reduced *CDKN1A* and *CDKN1C* (Figure 4CD), and had a small but non-significant effect on *CDKN2B* (Supplemental Figure 5A). To determine whether *CDKN1A* and/or *CDKN1C* reductions might underlie the synergistic effects of the TGFβSF inhibition in the harmine-TGFβSF inhibitor combination, we silenced *CDKN1A* and *CDKN1C* in human islets, either alone or in combination with harmine treatment (Figure 4E). As reported previously (Avrahami et al., 2014; Wang et al., 2017), *CDKN1C* silencing led to a modest increase in human beta cell proliferation, whereas silencing *CDKN1A* had no effect. In contrast, in the presence of harmine, silencing of either or both *CDKN1A* and *CDKN1C* led to robust human beta cell proliferation. Finally, to confirm whether or not *CDKN1A, CDKN1C* and *CDKN2B* truly function as cell cycle inhibitors in human beta cells, we overexpressed them in human islets treated with harmine and the TGFβ inhibitor, LY364947. Overexpression of each cell cycle inhibitor dramatically reduced proliferation in harmine-TGFβ inhibitor-treated human beta cells to rates approaching zero (Figure 4F).

Collectively, these observations suggest a mechanism for the synergistic effects of the harmine-TGFβ inhibitor combination on proliferation: harmine, through DYRK1A inhibition and nuclear NFAT retention (Demozay et al., 2011; Goodyer et al., 2012; Heit et al., 2006; Wang et al., 2015a), and likely other mechanisms discussed below, predominantly activates cell cycle genes; in a complimentary fashion, TGFβ inhibition, via attenuation of SMAD signaling, reduces expression of *CDKN2B, CDKN1A* and *CDKN1C*, each of which normally functions as a cell cycle inhibitor in human beta cells. This TGFβ inhibitor-mediated reduction in *CDKN2B, CDKN1A* and *CDKN1C*, synergizes with the harmine-induced, DYRK1A-mediated increases in cyclins and CDKs, permitting greater cell cycle activation than occurs via either harmine treatment or TGFβ inhibition alone.

Effects of R-SMADs and Trithorax Complex On Cell Cycle Inhibitors.

R-SMADs may transactivate or repress genes, and may do so in complexes that include Trithorax members (Antebi et al., 2017; Brown and Schneyer, 2010; Brown et al., 2014; Chandrasekharappa et al., 1997; Chen et al., 2011; Chen et al., 2009; Crabtree et al., 2001; Crabtree et al., 2003; Dhawan et al., 2016; Dhawan et al., 2009; El-Gohary et al., 2014; Gaarenstroom and Hill, 2014; Macias et al., 2015; Nomura et al., 2014; Smart et al., 2006; Stewart et al., 2015; Xiao et al., 2016; Xiao et al., 2014; Zhou et al., 2013). Both Trithorax and SMAD signaling have been implicated in beta cell proliferation in human insulinoma

(Wang et al., 2017). Thus, we queried whether R-SMADS 2,3 and/or 4 might directly interact with regulatory regions of the *CDKN1A* and/or *CDKN1C* genes in human islets (Figure 5AB). Indeed, SMADs 2/3 and 4 associate with promoter and enhancer regions of *CDKN1A* and *CDKN1C* (black bars in Figure 5CD) defined by Pasquali, Ferrer et al (Pasquali et al., 2014), and these associations were altered by treatment with the harmine-TGFβ inhibitor combination (white bars). Notably, MEN1, a Trithorax member and H3K4 methylase, was also observed to bind to some of these same regions in *CDKN1A* and *CDKN1C*, and these associations were also altered by harmine-TGFβ inhibitor treatment (Figure 5CD). Finally, the H3K27 demethylase, KDM6A, also a Trithorax member that binds specifically to the *CDKN1C* promoter in FACS-sorted human beta cells (Wang et al., 2017), co-localizes with MEN1 on the *CDKN1A* promoter in human islets, and this association is diminished by harmine-TGFβ inhibitor treatment (Figure 5C). Paradoxically, in contrast to results with MEN1, while KDM6A associates with the *CDKN1C* locus in human islets, this association appears to be enhanced rather than reduced with harmine-TGFβ inhibitor treatment (Figure 5D). Taken together, these observations make it clear that R-SMADs, MEN1 and KDM6A do indeed directly or indirectly bind to the regulatory regions of *CDKN1A* and *CDKN1C* in human islets, and do so in regions also occupied by Trithorax members. Importantly, these associations are disrupted by harmine-TGFβ inhibitor treatment. Collectively, these findings are consistent with a model (Figure 5EF) in which SMAD-Trithorax interactions maintain *CDKN1A* and *CDKN1C* expression in beta cells under basal circumstances, under the influence of TGFβSF-mediated SMAD signaling in coordination with a Trithorax-mediated open chromatin state at these loci. Following harmine-TGFβ inhibitor treatment, these complexes appear to dissociate or remodel, apparently disrupting SMAD-transactivation of the *CDKN1A* and *CDKN1C* loci.

Combined harmine-TGFβ inhibitor treatment enhances mouse and human beta cell proliferation and mouse beta cell expansion in vivo.

All of the preceding studies were performed in human islets *in vitro*. To determine whether comparable effects could be observed *in vivo*, we employed three models. First, we explored the combined effects of a maximally effective dose of harmine (10 mg/kg IP) (Wang et al., 2015a) with ALK5 inhibitor II, SB431542, LY364947 and GW788388, administered once per day for seven days, on Ki67 beta cell labeling in endogenous pancreatic beta cells of C57BL6 mice. Among these, the combination of harmine (10 mg/kg/day) together with GW788388 (30 mg/kg/day) proved most effective (Figure 6AB), and was selected for subsequent studies. As reported previously, harmine (Wang et al., 2015a) and TGFβSF inhibitors (Dhawan et al., 2016; Xiao et al., 2014; Zhou et al., 2013) individually induce proliferation in mouse beta cells *in vivo*. However, as observed *in vitro*, combined treatment *in vivo* with harmine and GW788388 produced a substantially larger effect than either alone, achieving an *in vivo* beta cell labeling index of 2%.

Second, to determine if the proliferation noted with Ki67 labeling might translate into actual beta cell regeneration *in vivo*, we used the partial (60%) pancreatectomy (PPX) mouse model (Figure 6C,D, **Supplemental Figures** 5B,6) (Wang et al., 2015a). Mice undergoing sham PPX showed no significant change in beta cell mass after seven days of treatment, although mice treated with the harmine-GW788388 combination appeared to be trending

upwards. Most importantly, beta cell mass had expanded significantly within seven days in mice that underwent a 60% PPX followed by the harmine-GW788388 combination. In contrast, the three control groups remained substantially below normal.

Finally, we queried whether systemic treatment with the harmine-GW788388 combination could enhance beta cell proliferation in transplanted human islets *in vivo* in the NOD-SCID mouse model (Figure 6E,F). As observed previously (Wang et al., 2015a), harmine treatment induced human beta cell proliferation *in vivo*, as did GW788388. Most notably, and as occurred with human beta cells *in vitro* and with mouse beta cells *in vivo*, treatment with the harmine-GW788388 combination was substantially more effective in driving human beta cell proliferation *in vivo* than either agent alone, yielding degrees of beta cell proliferation in transplanted human islets *in vivo* not previously observed by ourselves (Wang et al., 2015a) or others (Dhawan et al., 2016; Dirice et al., 2016) in response to any drug, nutrient or growth factor. Importantly, beta cells from four of the five islet donors displayed greater Ki67 immunolabeling in the harmine plus GW788388 group than in the three other groups.

Discussion

We provide a number of important new observations. First, we describe a novel combination of two distinct classes of molecules - a DYRK1A inhibitor combined with a TGFβ superfamily inhibitor - that reliably induces "rates" of proliferation in mature adult human beta cells averaging 5-8%, rates not previously been observed with any class of therapeutic molecules, and which far exceed normal physiological pancreatic beta cell replication in the first year of life (Gregg et al., 2012; Kassem et al., 2000; Meier et al., 2008; Wang et al., 2015b). Second, we illustrate that this is a class effect, achieved by many different DYRK1A inhibitors and many different TGFβ superfamily inhibitors. Third, we demonstrate that the DYRK1A inhibitor-TGFβSF inhibitor combination behaves synergistically, and provide novel mechanisms and models for this synergy (Figure 7A). Fourth, we demonstrate that beta cell numbers actually increase in three different models, two human and one murine. Fifth, we provide mechanistic explanations, using both pharmacologic and genetic approaches, for the concept that simultaneous inhibition of DYRK1A and SMAD signaling is both necessary and sufficient for the synergy. Sixth, we document that the beneficial effects on human proliferation are achieved in part via modulation of the activities of chromatin-modifying, epigenetic modulating enzymes of the Trithorax family, and extend Trithorax beta cell modulatory involvement to KDM6A and likely additional Trithorax members (Figure 7B). Seventh, we observe that beta cell proliferation generated by the harmine-TGFβSF inhibitor combination is not associated with beta cell de-differentiation, and instead favors maintained or increased beta cell differentiation. Eighth, the beneficial mitogenic and pro-differentiation effects of the DYRK1A inhibitor-TGFβSF inhibitor combination extend to beta cells from people with Type 2 diabetes. Ninth, we add leucettine-41 (Tahtouh et al., 2012) to the growing list of small molecule DYRK1A inhibitors that are able to activate human beta cell proliferation. Tenth, we extend the induction of proliferation *in vitro* to three distinct mouse and human *in vivo* models. Eleventh, the observations strongly suggest that locally produced endogenous TGFβSF agonists such as TGFβ's activins, inhibins, BMPs and related molecules play a key physiologic role in restraining beta cell mass expansion, and that this inhibitory pathway can

be manipulated for therapeutic purposes. Finally, while DYRK1A remains a central target of harmine and other DYRK1A inhibitors, we suggest that harmine also may act in part via SMAD pathways as well.

While DYRK1A inhibitors such as harmine, 5-IT, INDY, GNF4877 have been shown to induce replication in human beta cells, the "rates" of proliferation or labeling indices have been low, in the 1.5-3% range *in vitro* (Aamodt et al., 2016; Abdolazimi et al., 2018; Dirice et al., 2016; Shen et al., 2015; Wang et al., 2015a; Wang et al., 2016), and far lower in *in vivo* transplant models (Dirice et al., 2016; Wang et al., 2015a). Thus, while harmine analogue-induced beta cell proliferation is an important advance, one might envision higher rates of proliferation as being required for therapeutic human beta cell expansion in T1D and T2D. The average "rates" in the 5-8% range obtained with the DYRK1A inhibitor-TGFβ inhibitor combination (Figure 1,2) are notable in this regard.

TGFβ inhibitors and SMAD inhibition are well known as activators of proliferation in rodent islets (Brown and Schneyer, 2010; Brown et al., 2014; Dhawan et al., 2016; El-Gohary et al., 2014; Mukherjee et al., 2007; Nomura et al., 2014; Smart et al., 2006; Xiao et al., 2016; Xiao et al., 2014; Zhou et al., 2013). For example, Schneyer et al demonstrated in 2007 that knockout of the endogenous activin inhibitor, follistatin-like-3, leads to beta cell expansion in mouse genetic models (Mukherjee et al., 2007). Teramoto et al have reported that beta cell-specific disruption of *smad2* leads to beta cell hyperplasia (Nomura et al., 2014). Kim and Gittes have both reported that spontaneous or inducible upregulation of the I-SMAD, *smad7*, is associated with beta cell proliferation and expansion in mice (Smart et al., 2006; Xiao et al., 2016; Xiao et al., 2014). And Bhushan, Kulkarni et al have used small molecule TGFβ receptor inhibitors to activate proliferation in mouse pancreatic beta cells (Dhawan et al., 2016; Zhou et al., 2013). When examined in adult human islets, however, beta cell proliferation in response to TGFβSF inhibitors has been modest or negligible (Dhawan et al., 2016), a result we confirm (Figure 1A).

One important advance herein was to employ TGFβ inhibitors in combination with harmine, a concept we derived from human insulinoma data mining, wherein both DYRK1A and SMAD pathway abnormalities are evident (Wang et al., 2017). Moreover, we observe that inhibiting many of the various classes of TGFβ superfamily receptors, including TGFβ, activin and BMP receptors, in the presence of harmine, are all effective in permitting beta cell proliferation. We also find, as reported previously (Brown et al., 2014), that TGFβ superfamily members and SMAD signaling pathways are abundant in human islets. We infer that these collectively comprise an inhibitory regulatory network that restrains human beta cell proliferation, perhaps, as suggested by Gittes and Kim, to protect against de-differentiation (Smart et al., 2006; Xiao et al., 2016; Xiao et al., 2014), or perhaps against inappropriate beta cell expansion which might cause dangerous hypoglycemia, as occurs in insulinoma and congenital hyperinsulism. Importantly, the efficacy of the harmine-TGFβSF inhibitor combination translates from purely *in vitro* systems to three different *in vivo* models.

Another key advance is the demonstration that the increases in beta cell proliferation implied by elevated Ki67, BrdU and pHH3 labeling measures widely used in beta cell biology,

actually translate into increases in numbers of human beta cells. It has been challenging to demonstrate actual increases in human beta cell numbers in response to any agent. Laffitte observed an increase in human beta cell numbers *in vitro* in response to GNF4877 using advanced imaging techniques (Shen et al., 2015). Fiaschi-Taesch, using complex imaging and image analysis, also showed that cyclin and cyclin-dependent kinase overexpression using gene therapy approaches was able to increase human beta cell numbers (Tiwari et al., 2015). And Kerr-Conte et al suggested that transplanted human islet cell mass can increase in response to high fat feeding (Gargani et al., 2013). Each of these models is tedious and/or requires advanced imaging equipment, barriers to their widespread adoption. Not surprisingly, therefore, none of these approaches has been widely adopted. Here, we report a straightforward flow cytometric method to assess actual human beta cell numbers, and demonstrate its ease and efficacy in two different human beta cell models. Using this method, we find that adult beta cell numbers are approximately 50% higher in human islets treated for four days with the harmine-TGFβ inhibitor combination than control islets (Figure 1H). This is in the general range that might be anticipated with a proliferation rate of 5-8%. For example, one might predict conservatively that at a labeling index of 5-8%/day over four days would lead to a 22-36% increase in beta cell numbers. Along the same lines, in the Mel1-hESC cell experiments, which continued for seven days, one might assume a 50-70% increase in beta cell numbers, approximating the near doubling observed (Fig. 1I). Of course, these calculations are approximate and rely on imperfect assumptions, but may suggest that the Ki67 labeling indices actually underestimate the true rate of beta cell proliferation. Thus, alternately or in addition, they may reflect additional beneficial effects on beta cell survival, on enhanced beta cell differentiation and/or on transdifferentiation from other islet cell types. Whatever the mechanisms, increases in human beta cell numbers of this magnitude following four to seven days of treatment would be a welcome addition to the regenerative armamentarium.

We find that the DYRK1A inhibitor-TGFβSF inhibitor combination is not merely additive, but clearly synergistic (Figure 1, Supplemental Figure 1AB). Mechanistically, DYRK1A inhibitors seem to preferentially activate cell cycle activators, such as cyclins and cdks, whereas the TGFβSF inhibitors seem to preferentially repress cell cycle inhibitors, notably *CDKN1A, CDKN1C* and *CDKN2B*, effects that appear to be mediated, at least for *cDkNIA* and *CDKN1C*, by SMAD signaling and Trithorax chromatin remodeling. While we find clear evidence for TGFβ superfamily member effects being mediated by *CDKN1A* and *CDKN1C*, documenting involvement of *CDKN2B* and *CDKN2A* is more difficult because they arise from a common locus that encodes additional cell cycle modulators such as p14[ARF], ANRIL and others. These issues, and the unusually GC-rich nature of this locus, make selective silencing of *CDKN2A* and *CDKN2B* challenging. Finally, while the apparent complimentary actions of DYRK1A inhibitors and TGFβ superfamily inhibitors, illustrated in Figure 7A, likely explain much of the apparent synergy, they are unlikely the exclusive mechanism for the observed synergy, as evidenced by the ability of harmine alone to modulate expression and abundance of TGFβ superfamily members (Figure 3A, Supplemental Table 2). Indeed, several reports indicate that DYRK1A can phosphorylate a broad range of targets in addition to the NFaT family, including Tau, TP53, p27[CIP], and the DREAM complex member, LIN52 (Abdolazimi et al., 2018; Branca et al., 2017; Litovchick

et al., 2011; Park et al., 2010; Sadasivam and DeCaprio, 2013). We thus speculate that currently unknown additional targets likely exist that may lead to destabilization and/or dephosphorylation of SMADs as observed in Figure 3A. Clarification of these additional mechanisms in future studies is warranted.

The involvement of the Trithorax family of epigenetic modifying genes in controlling beta cell growth is not unexpected. The canonical Trithorax member, *MEN1*, was positionally cloned from people with the Multiple Endocrine Neoplasia type 1 syndrome (Chandrasekharappa et al., 1997), which includes insulinomas. MEN1, and other Trithorax members have been shown to regulate beta cell proliferation and mass in animal models and cell lines (Crabtree et al., 2001; Crabtree et al., 2003; Dhawan et al., 2016; Karnik et al., 2005; Zhou et al., 2013). Moreover, MEN1 and other Trithorax members, such as MLL's, have also been shown to participate in rodent beta cell proliferation and directly bind using ChIP to cell cycle inhibitor loci (Dhawan et al., 2016; Zhou et al., 2013). In addition, another Trithorax member, KDM6A, has recently been shown to be recurrently inactivated in human insulinomas (Wang et al., 2017); silencing or pharmacologically inhibiting KDM6A in human beta cells can block expression of the cell cycle inhibitor, *CDKN1C* (Wang et al., 2017). Here, we extend these observations by showing that the DYRK1A inhibitor-TGFβSF inhibitor combination disrupts normal physical interactions among MEN1 and KDM6A with *CDKN1A* and *CDKN1C* promoters and enhancers, and provide for the first time an example of harmine-TGFβSF inhibition modulating the binding of the canonical Trithorax member, MEN1 to regulatory regions of the key cell cycle inhibitor, *CDKN1C*, in human islets. Since these studies were performed in whole islets, additional studies will be required to elucidate which events actually occur in beta cells. Similarly, genome-wide studies such as ChIPseq and ATAC-seq using purified beta cells will be required to document and clarify specific interactions on a genome-wide basis

Accili and collaborators have reported that Type 2 diabetes in mouse and human beta cells is associated with de-differentiation to a more primitive, and poorly functional, insulin-depleted neuroendocrine cell type (Talchai et al., 2012). As was the case with harmine (Wang et al., 2015a), the harmine-TGFβSF inhibitor combination increased several key markers of human beta cell identity, differentiation and maturity, including *NKX6.1, PDX1, MAFA, MAFB, SLC2A2* and *PCSK1* (Figure 2A-C, Supplemental Table 2). We presume, but have not experimentally confirmed, that this relates in part to DYRK1A inhibition with resultant NFaT nuclear translocation and binding to promoters of this class of genes, as documented by Kim et al in mouse beta cells (Goodyer et al., 2012; Heit et al., 2006). The observation that some, but not all, presumptive beta cell differentiation factors are increased in human islets treated with the harmine-TGFβ inhibitor combination is reminiscent of observations of Sekine et al and Klochendler et al (Klochendler et al., 2016; Sekine et al., 1994) who observed that proliferating Ins1 cells (Sekine et al., 1994) or mouse beta cells (Klochendler et al., 2016) display varying effects on key beta cell functions, such as reducing lactate dehydrogenase (LDH) activity, and on transcriptomic readouts. For example, abundance of mRNAs encoding the key beta cell transcription factors *Nkx6.1, Mafa* and *Pdx1* remained normal in proliferating mouse beta cells, while transcripts encoding genes involved in secretory granule function such as secretogranin V (Scg5), Pcsk1, Vamp4, carboxypeptidase (Cpe) and Rab3a, were reduced. Clarifying such complex

events will require studies in single cells, at multiple time points, and in response to multiple treatments, and in islets from normals and people with T2D, employing technologies such as single cell RNAseq, CyTOF analysis, and microsecretion studies from individual beta cells. From a therapeutic standpoint, the fact that a differentiated molecular phenotype and glucose-stimulated insulin secretion remain intact despite induction of proliferation in normal (Figure 2A-D) and Type 2 diabetes islets (Figure 2EF) bodes well for treatment of people with Type 2 diabetes, and merits further exploration.

Limitations of This Study. A number of important additional challenges remain in the field of beta cell regenerative research. First, this study employed of islets from 104 different human islet donors, illustrating a major challenge the field or regenerative beta cell biology faces. The field lacks: easy and affordable access to large numbers of human islets, which themselves are remarkably heterogeneous; unequivocal, universally accepted approaches to high-throughput, high-precision human cadaveric beta cell drug screening and quantitation; and, perfect model cell lines with which to perform such studies.

Second, beta cell targeting remains a major challenge. Since SMAD and DYRK1A signaling are ubiquitous, the DYRK1A inhibitor-TGFβSF inhibitor strategy will certainly have off-target effects on many tissues, as illustrated by the CNS effects of harmine (Brierley and Davidson, 2012; Heise and Brooks, 2017), and the mitogenic effects of the harmine-TGFβSF inhibitor effects on alpha and ductal cells (Supplemental Figure 3). At this moment, there is no molecule that is able to target or deliver any drug specifically to the beta cell, an observation that has prompted urgent requests for such targeting molecules from diabetes funding agencies. Thus, one might envision a future in which drugs such as harmine and TGFβ inhibitors might be administered systemically and delivered directly and specifically to human beta cells - but not to other cell types - via carrier or transport molecules such as beta cell-specific GLP1 analogues, monoclonal antibodies, RNA aptamers, and/or zincophilic delivery molecules. Alternately, one might imagine using the drug combination to expand human islets *ex vivo* prior to transplantation.

A third concern relates to the potential long-term effect of TGFβSF inhibitors to cause de-differentiation in beta cells. Both Gittes and Kim have reported in mouse models that upregulation or overexpression of the I-SMAD, *smad7*, in beta cells over the longer term result in beta cell de-differentiation, but that re-differentiation occurs in association with termination of the SMAD7 signal (Smart et al., 2006; Xiao et al., 2016; Xiao et al., 2014). Teramoto et al report that knockout of the R-SMAD, *smad2*, also induces beta cell de-differentiation (Nomura et al., 2014). These observations predict that continuous long term TGFβSF inhibition may result in human beta cell de-differentiation, and that cyclical dosing strategies may be required, as is commonly employed with TGFβSF inhibitors in current clinical use (Cohn et al., 2014; Herbertz et al., 2015; Mascarenhas et al., 2014; Necchi et al., 2014; Trachtman et al., 2011; Yanagita, 2012). A third challenge is that proliferation rates appear less robust *in vivo* (~2%) than *in vitro* (~5-8%), a result that we speculate reflects the greater abundance of TGFβSF ligands in the *in vivo* environment versus *in vitro*. Of particular relevance here is the observation that the although TGFβ inhibitor GW788388 had no mitogenic effect on human beta cells *in vitro* (Figure 1A), it did increase proliferation *in vivo* (Figure 6E,F). This may provide additional support for the concept that endogenous

TGFβSF ligands serve as important *in vivo* physiologic repressors of adult human beta cell replication.

Finally, while these strategies appear to be promising for both Type 1 and Type 2 diabetes, they may be particularly attractive in Type 2 diabetes, since residual beta cell mass is substantially higher in Type 2 than in Type 1 diabetes, and since autoimmunity is not operative. Most important, these studies support the possibility that restorative treatment of beta cell deficiency and function in Type 1 and Type 2 diabetes is achievable.

STAR Methods

CONTACT FOR REAGENT AND RESOURCE SHARING

Requests for reagents and resources should be directed to, and will be fulfilled by, Dr. Andrew F. Stewart at 'andrew.stewart@mssm.edu'.

EXPERIMENTAL MODEL AND SUBJECT DETAILS

Human Pancreatic Islet Studies.—HIPPA-Compliant de-identified islets from 98 normal and six Type 2 diabetic adult cadaveric pancreas donors were obtained from the NIH/NIDDK-supported Integrated Islet Distribution Program (IIDP) (https://iidp.coh.org), from Dr. Tatsuya Kin at the University of Alberta, or from Dr. Patrick MacDonald at the Alberta Diabetes Institute. In all cases, informed written consent was provided at the institutions where the organs were harvested. For the normal doors, the mean age was 43.1 y.o. (range 16-68), 67 were male and 31 female, and the mean BMI was 30.5 (range 18.4-47.8). Sixty-six were Caucasian, 22 Hispanic/Latino, 6 Black, 3 Asian and 1 Pacific Islander. The mean cold ischemia time was 509 minutes (range 210-1340). Purity ranged from 55-99%. Among the Type 2 diabetes donors, the mean age was 53.8 y.o. (range 46-62), four were male and two were female, the mean BMI was 36.2 (range 32.5-42.8), and three were Caucasian and three were Hispanic. The mean HbA1c ($\pm$ SEM) was 8.8 ($\pm$ 3.9), and three had had T2D for 0-5 years while the other three had had T2D for 6-10 years. Five of the six were on diabetes medications (1 on insulin, 4 on metformin, and 1 on an unknown diabetes medication). The causes of death were stroke (4), head trauma (1) and anoxia (1). Mean cold ischemia time was 367 min (range 352-384 min). Islet purity ranged from 55-85%. Depending on the experiments performed, islets were used either as intact islets, or were first dispersed with Accutase (Sigma, St. Louis, MO) onto coverslips as described in the Figure Legends.

Mouse Studies.—All studies were approved in advance by, and performed in compliance with, the Icahn School of Medicine at Mount Sinai Institutional Animal Care and Use Committee. *Normal Mouse Pancreas Studies.* Male C57BL/6N mice (12-week-old) received vehicle (saline), 10 mg/kg harmine HCl, 30 mg/kg GW788388 or the combination of harmine and GW788388 by intraperitoneal injection daily for 7 days. Mice were sacrificed on day 7, pancreata harvested, fixed in 10% neutral buffered formalin, paraffin embedded and sectioned. Sections were stained for Ki67 and insulin as previously reported (Wang et al., 2015a). A minimum of 2,000 beta cells per pancreas was counted. *Mouse Partial Pancreatectomy (PPX) Studies.* These studies were performed exactly as described

previously (Wang et al., 2015a), with one exception: pancreas remnants were harvested at one week, rather than two weeks, following PPX. Briefly, 12 week old C57BL/6N mice underwent a sham or real 60% PPX. Seven days later, they were euthanized and the pancreas remnant harvested, weighed, fixed, sectioned, immunolabeled for insulin, beta cell area counted, and beta cell mass determined, all as described (Wang et al., 2015a). *NOD-SCID Mouse Studies.* Male NOD-SCID mice (12 week old) were transplanted with human cadaveric islets in the left renal subcapsular space as described previously (Wang et al., 2015a). On postoperative day 7, they were randomized to receive vehicle (saline), 10 mg/kg harmine HCl, 30 mg/kg GW788388 or the combination of harmine and GW788388 by intraperitoneal injection daily for seven days. The renal grafts then were harvested, fixed, sectioned, immunolabelled for insulin and Ki67, and counted as described above, and as reported (Wang et al., 2015a). Five human islet donors were used in each of five sets of four NOD-SCID mice. A minimum of 2000 human beta cells were counted per graft. Investigators were blinded as to group assignments in all studies.

METHOD DETAILS

Adenoviruses and Transduction.—Adenoviruses were prepared as described previously (Cozar-Castellano et al., 2004; Fiaschi-Taesch et al., 2009; Fiaschi-Taesch et al., 2013a; Fiaschi-Taesch et al., 2013b; Wang et al., 2017; Wang et al., 2015a). Unless otherwise described, all transductions were performed using 150 moi for two hours, and studies performed 96 hours later. The sequence and validation of the Ad.DYRK1A and Ad.shDYRK1A have been reported previously (Dirice et al., 2016; Wang et al., 2015a). Adenoviruses encoding human SMAD6 or SMAD7 were prepared using cDNAs encoding SMAD6 and SMAD7 obtained from Harvard PlasmID Database (https://plasmid.med.harvard.edu/). Adenoviruses employed for silencing SMADs 2,3 and 4 employed the DNA sequences in the Key Resources Table

Quantitative PCR.—RNA was isolated and quantitative RT-PCR was performed as described previously (Wang et al., 2015a). Gene expression in dispersed islets was analyzed by real-time PCR performed on an ABI 7500 System. Primers were as reported previously (Wang et al., 2015a) an in the Key Resources Table.

RNA sequencing.—RNA from whole human islets (**Supplemental Tables** 1,2) was prepared immediately using the RNeasy Micro kit (Qiagen). Beta cell RNA yields were 300-500 ng from each FACS run, and RNA integrity numbers were between 9.5 and 10.0. PolyA$^+$ mRNA from sorted beta cells was purified with oligo dT magnetic beads. The polyA$^+$ RNA from beta cells was then fragmented in the presence of divalent cations at 94°C. The fragmented RNA was converted into double stranded cDNA. After polishing the ends of the cDNA, the 3' ends were adenylated. Finally, Illumina-supplied universal adapters were ligated to the cDNA fragments. The adaptor ligated DNA was size selected to get an average of 250 bp insert size using AmpPure beads, and amplified by 15 cycle PCR. The PCR DNA was then purified using AmpPure beads to get the final seq library ready for sequencing. The insert size and DNA concentration of the seq library was determined on Agilent Bioanalyzer and Qubit, respectively. A pool of 10 barcoded RNA seq libraries was layered on two of the eight lanes of the Illumina flow cell at appropriate concentration and bridge amplified to

yield ~25- 35 million raw clusters. The DNA reads on the flow cell were then sequenced on HiSeq 2000 using a 100 bp paired end recipe. Results are expressed as millions of counts (reads) per million bases (CPM).

Immunocytochemistry.—Immunocytochemistry was performed on 4% paraformaldehyde fixed (15 min), Accutase-dispersed human islets plated on coverslips as described (Gaarenstroom and Hill, 2014; Micallef et al., 2012; Pagliuca et al., 2014; Tahtouh et al., 2012; Wang et al., 2015a; Wang et al., 2015b). Primary antisera are shown in the Key Resource Table. TUNEL labeling was performed as described (Gaarenstroom and Hill, 2014; Micallef et al., 2012; Pagliuca et al., 2014; Tahtouh et al., 2012; Wang et al., 2015a; Wang et al., 2015b).

Immunoblotting.—Immunoblots were performed on whole human islets as described in detail previously (Cozar-Castellano et al., 2004; Fiaschi-Taesch et al., 2009; Fiaschi-Taesch et al., 2013a; Fiaschi-Taesch et al., 2013b; Wang et al., 2015a).

Glucose-Stimulated Insulin Secretion.—GSIS was performed as described previously (Cozar-Castellano et al., 2004; Fiaschi-Taesch et al., 2009; Fiaschi-Taesch et al., 2013a; Fiaschi-Taesch et al., 2013b; Wang et al., 2015a). Briefly, whole human islets were cultured in low glucose (2.8mM) or high glucose (16.8 mM) for 30 min, and media harvested and assayed for insulin (Mercodia). Results are expressed as fold change in media insulin concentration in high glucose as compared to the low glucose concentration.

Proliferation in HUES8-Derived Human Beta Cells.—Stem cell-derived beta cell proliferation assays were performed using three separate batches of cryopreserved cells. Differentiation of Harvard University embryonic stem 8 (HUES8) cells into beta cells was carried out as previously described (Millman et al., 2016; Pagliuca et al., 2014). Briefly, cryobanked SC-islet cells were thawed and aggregated in Stage 6 (S6) media (DMEM/F12 plus 1% HSA) for 8 -11 days in suspension culture. Clusters were then dissociated using Accutase (Innovative Cell Technologies, catalog #: AT-104) for 10 mins and plated onto Matrigel- (Corning, catalog #: 354277) coated 96 well plates at a density of 1×10^5 cells/ well in S6 media with 10 uM Y-27632. Following 24 hrs of culture, compound treatment was initiated and lasted for four days with replenishment every other day. Cells were fixed with 4% paraformaldehyde for 15 mins then stained overnight for insulin (Dako, A0564) and Ki67 (Thermo Scientific, RM-9106-s1) followed by fluorescent secondary antibodies (Thermo), anti-rabbit Alexa 594 and anti-guinea pig Alexa 488 and Hoescht (Thermo, H3569) staining. Beta cell proliferation (%insulin$^+$/Ki67$^+$) was quantified using a Multiwavelength Cell Scoring algorithm on the ImageXpress Micro 4 High-Content Imaging System (Molecular Devices) (Shen et al., 2015).

Expansion and Differentiation of Mel1-Derived Beta Cells: Stem cell line and culture.—The Mel1 hESC line (Micallef et al., 2012) used in this manuscript is an NIH approved line (registry # 0139). hESC are grown on plates coated with primary mouse embryonic fibroblasts or MEFs (GlobalStem, CF-1 MEF IRR) and using human ES medium containing DMEM (Gibco, 10569), 10% FBS (GE Healthcare, SH30088.03HI), 1% GlutaMAX (Gibco, 35050061) and 1% Pen-Strep (Thermo Fisher Scientific, 15070-063).

Cells are dissociated every 4-5 days using TrypLE™ Express (Life Technology, 12605036) for passaging. After dissociation, cells were suspended in human ES medium containing 10 μM ROCK inhibitor Y27632 (Selleckchem, S1049).

Differentiation of Mel1 Cells into Pancreatic Islets.—Cells are grown to 80-90% confluence, dissociated and suspended in mTeSR™ medium (STEMCELL Technology, 05850) with 10 μM ROCK inhibitor Y27632 (Selleckchem, S1049) and plated in a 1:1 ratio into Matrigel-coated (Fisher Scientific, 354277) wells for differentiation as previously described (Sui et al., 2018). The initial stages of differentiation were conducted in planar culture (d0-d11). For definitive endoderm stage (d1-d3) cells were cultured using STEMdiff™ Definitive Endoderm Differentiation Kit (Stemcell Technologies, 05110). For primitive gut stage (d4-d6), cells were cultured in RPMI containing GlutaMAX (Life Technology, 61870-127), 1% (v/v) Penicillin-Streptomycin (PS) (Thermo Fisher Scientific, 15070-063), 1% (v/v) B27 Serum-Free Supplement (50×) (Life Technology, 17504044) and 50 ng/ml FGF7 (R&D System, 251-KG). For posterior foregut stage (d7-d8), cells were cultured in DMEM containing GlutaMax, 1% (v/v) PS, 1% (v/v) B27, 0.25 μM KAAD-Cyclopamine (Stemgent, 04-0028), 2 μM Retinoic acid (Stemgent, 04-0021) and 0.25 μM LDN193189 (Stemgent, 04-0074). For pancreatic progenitor stage (d9-d11), cells were cultured in DMEM containing GlutaMax, 1% (v/v) PS, 1% (v/v) B27 and 50 ng/ml EGF (R&D System, 236-EG). Cells were then dissociated using TrypLE™ Express (Life Technology, 12605036) and seeded into low-attachment 96 well-plates (Corning, 7007) (1 well of 6 well-plate to 60 wells of 96-well-plate) for clustering step to form aggregates or clusters of endocrine cells in DMEM containing GlutaMax, 1% (v/v) PS, 1% (v/v) B27, 0.25 μM Cyclopamine, 1 μM thyroid hormone (T3) (Sigma, T6397), 10 μM Alk5i, 10 μM Zinc sulfate (Sigma-Aldrich, Z4750) and 10 μg/ml Heparin (Sigma-Aldrich, H3149) for 2 days (d12-d13). For pancreatic endocrine stage (d14-20) cells were cultured using DMEM containing GlutaMax, 1% (v/v) PS, 1% (v/v) B27, 100 nM LDN, 1 μM T3, 10 μM Alk5i, 10 μM Zinc sulfate, 10 μg/ml Heparin and 100 nM gamma-secretase inhibitor (DBZ) (EMD Millipore, 565789). For mature pancreatic endocrine stage (d21-d27) cells were cultured using DMEM containing GlutaMax, 1% (v/v) PS, 1% (v/v) B27, 1 μM T3, 10 μM Alk5i, 10 μM Zinc sulfate, 10 μg/ml Heparin, 1 mM N-acetyl cysteine (N-Cys) (Sigma-Aldrich, A9165-5G), 10 μM Trolox (EMD Millipore, 648471-500MG) and 2 μM R428 (Tyrosine kinase receptor AXL inhibitor) (ApexBio, A8329). From d1 to d11 media was changed every day and from d12 to d27 media was changed every other day. All differentiations were done for 27 to 30 days. At Day 21, beta cell clusters were dissociated with trypsin and seeded at the exact same cell number (300-500,000 cells per well) into chambers on poly-D-lysine/laminin-coated slides and treated with either DMSO or the harmine-TGFβ inhibitor combination.

Flow Cytometry to Quantify Human Beta Cells.—Human islets (250-300 IEQ) or stem cell-derived beta cells (300-500,000) were dispersed using Accutase (MT25058CI, Fisher Scientific) (for human islets) or trypsin (for hESC-derived beta cells) and plated on laminin/poly-D-lysine coated chamber slides (BD354688, VWR Scientific). For human islets, beta cells were labeled with an adenovirus as described previously (Wang et al., 2017). Briefly, human islet cells were dispersed to single cells in eigth-well chambers and

transduced for two hours in RPMI1640 medium without fetal bovine serum (FBS) with 150 moi of an adenovirus expressing the bright green fluorescent protein, ZsGreen (Clontech, Mountain View CA), under control of the rat insulin-1 promoter (RIP1) and a mini-CMV enhancer (Wang et al., 2017). The RIP1-miniCMV promoter included 177 bases of the hCMV IE-1 promoter ClaI-SpeI fragment ligated to 438 bases of the RIP1 promoter. The beta cell fraction was confirmed to be >92% pure by immunolabeling of sorted cells with insulin, by qRT-PCR and by RNAseq (Supplementary Figure 7) (Wang et al., 2017). Following transduction with the Ad.RIP-ZsGreen adenovirus for two hours, 300 μl of RPMI1640 medium containing 10% FBS was added to terminate adenovirus infection, and cells were allowed to express ZsGreen for 24 hours. At this point, fresh medium containing DMSO or harmine 10μM, Ly364947 3μM or the harmine-LY combination was added for another four days. Human Mel1-ES cell-derived beta cells were labeled with endogenous GFP (Sui et al., 2018).

For flow cytometric human beta cell quantification, following four days (for human islet cells) or seven days (for hESC-derived beta cells) of drug treatment (DMSO or harmine + LY364947), cells were harvested by gentle Accutase (for human beta cells) or trypsin (for hESC-dervied beta cells) dissociation and 50,000 fluorescent beads (ACURFP-50-10, Spherotech, Inc.) were added, serving as an internal recovery standard and FACS counting reference. DAPI (D3571, Life Technologies) was used as a dead/live cell marker. Dispersed cells were loaded onto an Aria II cell sorter, and live ZsGreen[+] (from human islets) or GFP[+] (from hESC) cells were counted until 10,000 beads had been counted from each the vehicle- and the harmine-LY364947-treated wells. Results are expressed as absolute numbers of ZsGreen[+] or GFP^{+} beta cells, corrected to the 50,000 original internal bead standard. The beta cell fraction was confirmed to be >92% pure by immunolabeling of sorted cells with insulin, by qRT-PCR and by RNAseq (Wang et al., 2017).

Chromatin Immunoprecipitation (ChIP) Assays.—ChIP was performed using the EZ-ChIP Kit (#Magna0001, Millipore) according to manufacturer's protocol as described previously (Wang et al., 2017). Whole human cadaveric islets were dispersed as described previously. A minimum of three separate islet preparations were used for each figure shown. 2×10^6 cells were collected per experiment for each SMAD2/3, SMAD4, KDM6A and MEN1 immunoprecipitation. Immunoprecipitated DNA was quantified using ABI 7500 real-time quantitative PCR detection system (Life Technologies). Data are presented as binding signals calculated by normalizing the ChIP signals relative to input controls and subsequently subtracting the IgG value from the respective antibody. The resulting values below zero indicated no binding and depicted as 'zero' in ChIP plots. Error bars indicate mean ± SEM. The primer sets for *CDKN1A* and *CDKN1C* were described previously (Koinuma et al., 2009; Wang et al., 2017; Yang et al., 2009). The antibodies and the primer sequences used are described in the Key Resources Table.

QUANTIFICATION AND STATISTICAL ANALYSIS

Statistics.—Statistics were performed using Student's two-tailed paired T-test (for paired samples) or by One-Way Analysis of Variance for repeated measures for multiple

comparisons, as described in the Figure Legends. P values less than 0.05 were considered to be significant.

DATA AND SOFTWARE AVAILIBILITY

RNAseq data re available in **Supplemental Tables** 1 and 2.

ADDITIONAL RESOURCES

Not Applicable

Supplementary Material

Refer to Web version on PubMed Central for supplementary material.

Acknowledgements

References

Aamodt KI, Aramandla R, Brown JJ, Fiaschi-Taesch N, Wang P, Stewart AF, Brissova M, and Powers AC (2016). Development of a reliable automated screening system to identify small molecules and biologics that promote human beta-cell regeneration. American journal of physiology. Endocrinology and metabolism 311, E859–E868. [PubMed: 27624103]

Abdolazimi Y, Lee S, Xu H, Allegretti P, Horton TM, Yeh B, Moeller HP, Nichols RJ, McCutcheon D, Shalizi A, et al. (2018). CC-401 Promotes beta-Cell Replication via Pleiotropic Consequences of DYRK1A/B Inhibition. Endocrinology.

Antebi YE, Linton JM, Klumpe H, Bintu B, Gong M, Su C, McCardell R, and Elowitz MB (2017). Combinatorial Signal Perception in the BMP Pathway. Cell 170, 1184–1196 e1124. [PubMed: 28886385]

Avrahami D, Li C, Yu M, Jiao Y, Zhang J, Naji A, Ziaie S, Glaser B, and Kaestner KH (2014). Targeting the cell cycle inhibitor p57Kip2 promotes adult human beta cell replication. The Journal of clinical investigation 124, 670–674. [PubMed: 24430183]

Branca C, Shaw DM, Belfiore R, Gokhale V, Shaw AY, Foley C, Smith B, Hulme C, Dunckley T, Meechoovet B, et al. (2017). Dyrk1 inhibition improves Alzheimer's disease-like pathology. Aging cell 16, 1146–1154. [PubMed: 28779511]

Brierley DI, and Davidson C (2012). Developments in harmine pharmacology--implications for ayahuasca use and drug-dependence treatment. Progress in neuropsychopharmacology & biological psychiatry 39, 263–272.

Brown ML, and Schneyer AL (2010). Emerging roles for the TGFbeta family in pancreatic beta-cell homeostasis. Trends in endocrinology and metabolism: TEM 21, 441–448. [PubMed: 20382030]

Brown ML, Ungerleider N, Bonomi L, Andrzejewski D, Burnside A, and Schneyer A (2014). Effects of activin A on survival, function and gene expression of pancreatic islets from non-diabetic and diabetic human donors. Islets 6, e1017226. [PubMed: 25833251]

Chandrasekharappa SC, Guru SC, Manickam P, Olufemi SE, Collins FS, Emmert-Buck MR, Debelenko LV, Zhuang Z, Lubensky IA, Liotta LA, et al. (1997). Positional cloning of the gene for multiple endocrine neoplasia-type 1. Science 276, 404–407. [PubMed: 9103196]

Chen H, Gu X, Liu Y, Wang J, Wirt SE, Bottino R, Schorle H, Sage J, and Kim SK (2011). PDGF signalling controls age-dependent proliferation in pancreatic beta-cells. Nature 478, 349–355. [PubMed: 21993628]

Chen H, Gu X, Su IH, Bottino R, Contreras JL, Tarakhovsky A, and Kim SK (2009). Polycomb protein Ezh2 regulates pancreatic beta-cell Ink4a/Arf expression and regeneration in diabetes mellitus. Genes & development 23, 975–985. [PubMed: 19390090]

Cinti F, Bouchi R, Kim-Muller JY, Ohmura Y, Sandoval PR, Masini M, Marselli L, Suleiman M, Ratner LE, Marchetti P, et al. (2016). Evidence of beta-Cell Dedifferentiation in Human Type 2 Diabetes. The Journal of clinical endocrinology and metabolism 101, 1044–1054. [PubMed: 26713822]

Cohn A, Lahn MM, Williams KE, Cleverly AL, Pitou C, Kadam SK, Farmen MW, Desaiah D, Raju R, Conkling P, et al. (2014). A phase I dose-escalation study to a predefined dose of a transforming growth factor-beta1 monoclonal antibody (TbetaM1) in patients with metastatic cancer. International journal of oncology 45, 2221–2231. [PubMed: 25270361]

Cozar-Castellano I, Takane KK, Bottino R, Balamurugan AN, and Stewart AF (2004). Induction of beta-cell proliferation and retinoblastoma protein phosphorylation in rat and human islets using adenovirus-mediated transfer of cyclin-dependent kinase-4 and cyclin D1. Diabetes 53, 149–159. [PubMed: 14693709]

Crabtree JS, Scacheri PC, Ward JM, Garrett-Beal L, Emmert-Buck MR, Edgemon KA, Lorang D, Libutti SK, Chandrasekharappa SC, Marx SJ, et al. (2001). A mouse model of multiple endocrine neoplasia, type 1, develops multiple endocrine tumors. Proceedings of the National Academy of Sciences of the United States of America 98, 1118–1123. [PubMed: 11158604]

Crabtree JS, Scacheri PC, Ward JM, McNally SR, Swain GP, Montagna C, Hager JH, Hanahan D, Edlund H, Magnuson MA, et al. (2003). Of mice and MEN1: Insulinomas in a conditional mouse knockout. Molecular and cellular biology 23, 6075–6085. [PubMed: 12917331]

Demozay D, Tsunekawa S, Briaud I, Shah R, and Rhodes CJ (2011). Specific glucoseinduced control of insulin receptor substrate-2 expression is mediated via Ca2+-dependent calcineurin/NFAT signaling in primary pancreatic islet beta-cells. Diabetes 60, 2892–2902. [PubMed: 21940781]

Dhawan S, Dirice E, Kulkarni RN, and Bhushan A (2016). Inhibition of TGF-beta Signaling Promotes Human Pancreatic beta-Cell Replication. Diabetes 65, 1208–1218. [PubMed: 26936960]

Dhawan S, Tschen SI, and Bhushan A (2009). Bmi-1 regulates the Ink4a/Arf locus to control pancreatic beta-cell proliferation. Genes & development 23, 906–911. [PubMed: 19390085]

Dirice E, Walpita D, Vetere A, Meier BC, Kahraman S, Hu J, Dancik V, Burns SM, Gilbert TJ, Olson DE, et al. (2016). Inhibition of DYRK1A Stimulates Human beta-Cell Proliferation. Diabetes 65, 1660–1671. [PubMed: 26953159]

El-Gohary Y, Tulachan S, Wiersch J, Guo P, Welsh C, Prasadan K, Paredes J, Shiota C, Xiao X, Wada Y, et al. (2014). A smad signaling network regulates islet cell proliferation. Diabetes 63, 224–236. [PubMed: 24089514]

Fiaschi-Taesch N, Bigatel TA, Sicari B, Takane KK, Salim F, Velazquez-Garcia S, Harb G, Selk K, Cozar-Castellano I, and Stewart AF (2009). Survey of the human pancreatic beta-cell G1/S proteome reveals a potential therapeutic role for cdk-6 and cyclin D1 in enhancing human beta-cell replication and function in vivo. Diabetes 58, 882–893. [PubMed: 19136653]

Fiaschi-Taesch NM, Kleinberger JW, Salim FG, Troxell R, Wills R, Tanwir M, Casinelli G, Cox AE, Takane KK, Scott DK, et al. (2013a). Human pancreatic beta-cell G1/S molecule cell cycle atlas. Diabetes 62, 2450–2459. [PubMed: 23493570]

Fiaschi-Taesch NM, Kleinberger JW, Salim FG, Troxell R, Wills R, Tanwir M, Casinelli G, Cox AE, Takane KK, Srinivas H, et al. (2013b). Cytoplasmic-nuclear trafficking of G1/S cell cycle molecules and adult human beta-cell replication: a revised model of human beta-cell G1/S control. Diabetes 62, 2460–2470. [PubMed: 23493571]

Gaarenstroom T, and Hill CS (2014). TGF-beta signaling to chromatin: how Smads regulate transcription during self-renewal and differentiation. Seminars in cell & developmental biology 32, 107–118. [PubMed: 24503509]

Gargani S, Thevenet J, Yuan JE, Lefebvre B, Delalleau N, Gmyr V, Hubert T, Duhamel A, Pattou F, and Kerr-Conte J (2013). Adaptive changes of human islets to an obesogenic environment in the mouse. Diabetologia 56, 350–358. [PubMed: 23192693]

Goodyer WR, Gu X, Liu Y, Bottino R, Crabtree GR, and Kim SK (2012). Neonatal beta cell development in mice and humans is regulated by calcineurin/NFAT. Developmental cell 23, 21–34. [PubMed: 22814600]

Gregg BE, Moore PC, Demozay D, Hall BA, Li M, Husain A, Wright AJ, Atkinson MA, and Rhodes CJ (2012). Formation of a human beta-cell population within pancreatic islets is set early in life. The Journal of clinical endocrinology and metabolism 97, 3197–3206. [PubMed: 22745242]

Heise CW, and Brooks DE (2017). Ayahuasca Exposure: Descriptive Analysis of Calls to US Poison Control Centers from 2005 to 2015. Journal of medical toxicology : official journal of the American College of Medical Toxicology 13, 245–248. [PubMed: 27896660]

Heit JJ, Apelqvist AA, Gu X, Winslow MM, Neilson JR, Crabtree GR, and Kim SK (2006). Calcineurin/NFAT signalling regulates pancreatic beta-cell growth and function. Nature 443, 345–349. [PubMed: 16988714]

Herbertz S, Sawyer JS, Stauber AJ, Gueorguieva I, Driscoll KE, Estrem ST, Cleverly AL, Desaiah D, Guba SC, Benhadji KA, et al. (2015). Clinical development of galunisertib (LY2157299 monohydrate), a small molecule inhibitor of transforming growth factor-beta signaling pathway. Drug design, development and therapy 9, 4479–4499.

Karnik SK, Hughes CM, Gu X, Rozenblatt-Rosen O, McLean GW, Xiong Y, Meyerson M, and Kim SK (2005). Menin regulates pancreatic islet growth by promoting histone methylation and expression of genes encoding p27Kip1 and p18INK4c. Proceedings of the National Academy of Sciences of the United States of America 102, 14659–14664. [PubMed: 16195383]

Kassem SA, Ariel I, Thornton PS, Scheimberg I, and Glaser B (2000). Beta-cell proliferation and apoptosis in the developing normal human pancreas and in hyperinsulinism of infancy. Diabetes 49, 1325–1333. [PubMed: 10923633]

Klochendler A, Caspi I, Corem N, Moran M, Friedlich O, Elgavish S, Nevo Y, Helman A, Glaser B, Eden A, et al. (2016). The Genetic Program of Pancreatic beta-Cell Replication In Vivo. Diabetes 65, 2081–2093. [PubMed: 26993067]

Koinuma D, Tsutsumi S, Kamimura N, Imamura T, Aburatani H, and Miyazono K (2009). Promoter-wide analysis of Smad4 binding sites in human epithelial cells. Cancer science 100, 2133–2142. [PubMed: 19686287]

Litovchick L, Florens LA, Swanson SK, Washburn MP, and DeCaprio JA (2011). DYRK1A protein kinase promotes quiescence and senescence through DREAM complex assembly. Genes & development 25, 801–813. [PubMed: 21498570]

Macias MJ, Martin-Malpartida P, and Massague J (2015). Structural determinants of Smad function in TGF-beta signaling. Trends in biochemical sciences 40, 296–308. [PubMed: 25935112]

Mascarenhas J, Li T, Sandy L, Newsom C, Petersen B, Godbold J, and Hoffman R (2014). Anti-transforming growth factor-beta therapy in patients with myelofibrosis. Leukemia & lymphoma 55, 450–452. [PubMed: 23682558]

Meier JJ, Butler AE, Saisho Y, Monchamp T, Galasso R, Bhushan A, Rizza RA, and Butler PC (2008). Beta-cell replication is the primary mechanism subserving the postnatal expansion of beta-cell mass in humans. Diabetes 57, 1584–1594. [PubMed: 18334605]

Micallef SJ, Li X, Schiesser JV, Hirst CE, Yu QC, Lim SM, Nostro MC, Elliott DA, Sarangi F, Harrison LC, et al. (2012). INS(GFP/w) human embryonic stem cells facilitate isolation of in vitro derived insulin-producing cells. Diabetologia 55, 694–706. [PubMed: 22120512]

Millman JR, Xie C, Van Dervort A, Gurtler M, Pagliuca FW, and Melton DA (2016). Generation of stem cell-derived beta-cells from patients with type 1 diabetes. Nature communications 7, 11463.

Mukherjee A, Sidis Y, Mahan A, Raher MJ, Xia Y, Rosen ED, Bloch KD, Thomas MK, and Schneyer AL (2007). FSTL3 deletion reveals roles for TGF-beta family ligands in glucose and fat

homeostasis in adults. Proceedings of the National Academy of Sciences of the United States of America 104, 1348–1353. [PubMed: 17229845]

Necchi A, Giannatempo P, Mariani L, Fare E, Raggi D, Pennati M, Zaffaroni N, Crippa F, Marchiano A, Nicolai N, et al. (2014). PF-03446962, a fully-human monoclonal antibody against transforming growth-factor beta (TGFbeta) receptor ALK1, in pre-treated patients with urothelial cancer: an open label, single-group, phase 2 trial. Investigational new drugs 32, 555–560. [PubMed: 24566706]

Nomura M, Zhu HL, Wang L, Morinaga H, Takayanagi R, and Teramoto N (2014). SMAD2 disruption in mouse pancreatic beta cells leads to islet hyperplasia and impaired insulin secretion due to the attenuation of ATP-sensitive K+ channel activity. Diabetologia 57, 157–166. [PubMed: 24068386]

Pagliuca FW, Millman JR, Gurtler M, Segel M, Van Dervort A, Ryu JH, Peterson QP, Greiner D, and Melton DA (2014). Generation of functional human pancreatic beta cells in vitro. Cell 159, 428–439. [PubMed: 25303535]

Park J, Oh Y, Yoo L, Jung MS, Song WJ, Lee SH, Seo H, and Chung KC (2010). Dyrk1A phosphorylates p53 and inhibits proliferation of embryonic neuronal cells. The Journal of biological chemistry 285, 31895–31906. [PubMed: 20696760]

Pasquali L, Gaulton KJ, Rodriguez-Segui SA, Mularoni L, Miguel-Escalada I, Akerman I, Tena JJ, Moran I, Gomez-Marin C, van de Bunt M, et al. (2014). Pancreatic islet enhancer clusters enriched in type 2 diabetes risk-associated variants. Nature genetics 46, 136–143. [PubMed: 24413736]

Pullen TJ, and Rutter GA (2013). When less is more: the forbidden fruits of gene repression in the adult beta-cell. Diabetes, obesity & metabolism 15, 503–512.

Sadasivam S, and DeCaprio JA (2013). The DREAM complex: master coordinator of cell cycle-dependent gene expression. Nature reviews. Cancer 13, 585–595.

Schuit F, Van Lommel L, Granvik M, Goyvaerts L, de Faudeur G, Schraenen A, and Lemaire K (2012). beta-cell-specific gene repression: a mechanism to protect against inappropriate or maladjusted insulin secretion? Diabetes 61, 969–975. [PubMed: 22517647]

Sekine N, Cirulli V, Regazzi R, Brown LJ, Gine E, Tamarit-Rodriguez J, Girotti M, Marie S, MacDonald MJ, Wollheim CB, et al. (1994). Low lactate dehydrogenase and high mitochondrial glycerol phosphate dehydrogenase in pancreatic beta-cells. Potential role in nutrient sensing. The Journal of biological chemistry 269, 4895–4902. [PubMed: 8106462]

Shen W, Taylor B, Jin Q, Nguyen-Tran V, Meeusen S, Zhang YQ, Kamireddy A, Swafford A, Powers AF, Walker J, et al. (2015). Inhibition of DYRK1A and GSK3B induces human beta-cell proliferation. Nature communications 6, 8372.

Smart NG, Apelqvist AA, Gu X, Harmon EB, Topper JN, MacDonald RJ, and Kim SK (2006). Conditional expression of Smad7 in pancreatic beta cells disrupts TGF-beta signaling and induces reversible diabetes mellitus. PLoS biology 4, e39. [PubMed: 16435884]

Stewart AF, Hussain MA, Garcia-Ocana A, Vasavada RC, Bhushan A, Bernal-Mizrachi E, and Kulkarni RN (2015). Human beta-cell proliferation and intracellular signaling: part 3. Diabetes 64, 1872–1885. [PubMed: 25999530]

Sui L, Danzl N, Campbell SR, Viola R, Williams D, Xing Y, Wang Y, Phillips N, Poffenberger G, Johannesson B, et al. (2018). beta-Cell Replacement in Mice Using Human Type 1 Diabetes Nuclear Transfer Embryonic Stem Cells. Diabetes 67, 26–35. [PubMed: 28931519]

Tahtouh T, Elkins JM, Filippakopoulos P, Soundararajan M, Burgy G, Durieu E, Cochet C, Schmid RS, Lo DC, Delhommel F, et al. (2012). Selectivity, cocrystal structures, and neuroprotective properties of leucettines, a family of protein kinase inhibitors derived from the marine sponge alkaloid leucettamine B. Journal of medicinal chemistry 55, 9312–9330. [PubMed: 22998443]

Talchai C, Xuan S, Lin HV, Sussel L, and Accili D (2012). Pancreatic beta cell dedifferentiation as a mechanism of diabetic beta cell failure. Cell 150, 1223–1234. [PubMed: 22980982]

Tiwari S, Roel C, Wills R, Casinelli G, Tanwir M, Takane KK, and Fiaschi-Taesch NM (2015). Early and Late G1/S Cyclins and Cdks Act Complementarily to Enhance Authentic Human beta-Cell Proliferation and Expansion. Diabetes 64, 3485–3498. [PubMed: 26159177]

Trachtman H, Fervenza FC, Gipson DS, Heering P, Jayne DR, Peters H, Rota S, Remuzzi G, Rump LC, Sellin LK, et al. (2011). A phase 1, single-dose study of fresolimumab, an anti-TGF-beta

antibody, in treatment-resistant primary focal segmental glomerulosclerosis. Kidney international 79, 1236–1243. [PubMed: 21368745]

Wang H, Bender A, Wang P, Karakose E, Inabnet WB, Libutti SK, Arnold A, Lambertini L, Stang M, Chen H, et al. (2017). Insights into beta cell regeneration for diabetes via integration of molecular landscapes in human insulinomas. Nature communications 8, 767.

Wang P, Alvarez-Perez JC, Felsenfeld DP, Liu H, Sivendran S, Bender A, Kumar A, Sanchez R, Scott DK, Garcia-Ocana A, et al. (2015a). A high-throughput chemical screen reveals that harmine-mediated inhibition of DYRK1A increases human pancreatic beta cell replication. Nature medicine 21, 383–388.

Wang P, Fiaschi-Taesch NM, Vasavada RC, Scott DK, Garcia-Ocana A, and Stewart AF (2015b). Diabetes mellitus--advances and challenges in human beta-cell proliferation. Nature reviews. Endocrinology 11, 201–212. [PubMed: 25687999]

Wang YJ, Golson ML, Schug J, Traum D, Liu C, Vivek K, Dorrell C, Naji A, Powers AC, Chang KM, et al. (2016). Single-Cell Mass Cytometry Analysis of the Human Endocrine Pancreas. Cell metabolism 24, 616–626. [PubMed: 27732837]

Xiao X, Fischbach S, Song Z, Gaffar I, Zimmerman R, Wiersch J, Prasadan K, Shiota C, Guo P, Ramachandran S, et al. (2016). Transient Suppression of TGFbeta Receptor Signaling Facilitates Human Islet Transplantation. Endocrinology 157, 1348–1356. [PubMed: 26872091]

Xiao X, Gaffar I, Guo P, Wiersch J, Fischbach S, Peirish L, Song Z, El-Gohary Y, Prasadan K, Shiota C, et al. (2014). M2 macrophages promote beta-cell proliferation by up-regulation of SMAD7. Proceedings of the National Academy of Sciences of the United States of America 111, E1211–1220. [PubMed: 24639504]

Yanagita M (2012). Inhibitors/antagonists of TGF-beta system in kidney fibrosis. Nephrology, dialysis, transplantation : official publication of the European Dialysis and Transplant Association - European Renal Association 27, 3686–3691.

Yang X, Karuturi RK, Sun F, Aau M, Yu K, Shao R, Miller LD, Tan PB, and Yu Q (2009). CDKN1C (p57) is a direct target of EZH2 and suppressed by multiple epigenetic mechanisms in breast cancer cells. PloS one 4, e5011. [PubMed: 19340297]

Zhou JX, Dhawan S, Fu H, Snyder E, Bottino R, Kundu S, Kim SK, and Bhushan A (2013). Combined modulation of polycomb and trithorax genes rejuvenates beta cell replication. The Journal of clinical investigation 123, 4849–4858. [PubMed: 24216481]

Highlights:

- Adult human pancreatic beta cells can be induced to proliferate at high rates.

- Driven by synergy between DYRK1A inhibitors and TGFβ superfamily inhibitors.

- Reflects activation of cyclins and CDKs accompanied by CDK inhibitor suppression.

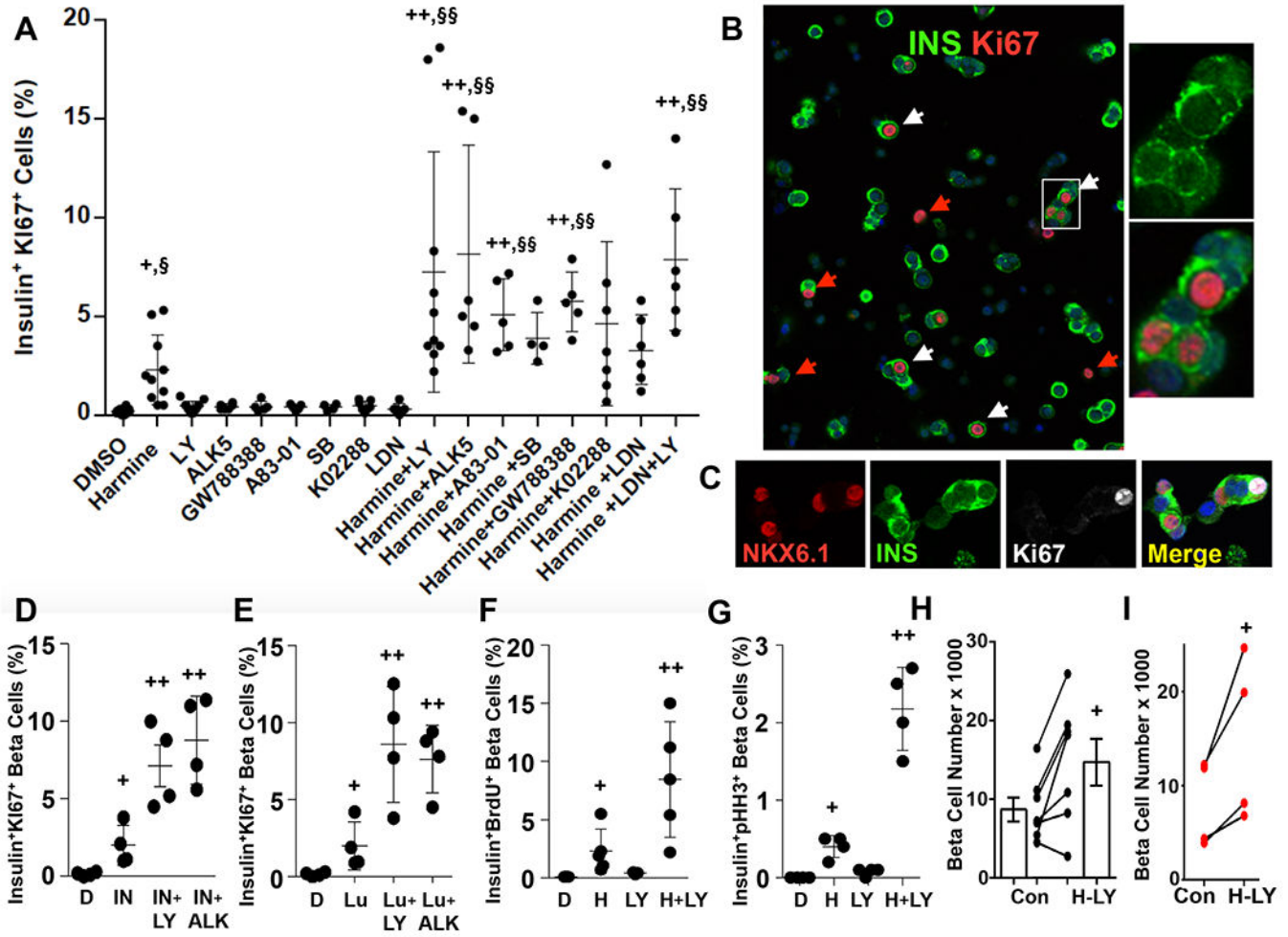- Proliferation occurs in Type 2 diabetic beta cells, with enhanced differentiation.

Figure 1. Induction of human beta cell proliferation and augmentation of beta cell numbers by combined harmine and TGFβSF inhibitor treatment.

A. The effects of harmine alone, and of various TGFβSF ligand inhibitors, some of which are specific for TGFβ receptors, and others for activin, inhibin and BMP receptors. As can be seen, and as reported previously (Aamodt et al., 2016; Abdolazimi et al., 2018; Dirice et al., 2016; Shen et al., 2015; Wang et al., 2015a; Wang et al., 2016), harmine induces Ki67 labeling in approximately 2% of normal human beta cells, and TGFβSF inhibitors lead to only marginal Ki67 labeling. However, each of the TGFβSF inhibitors in combination with harmine induces striking increases in Ki67 labeling in beta cells. **B.** Examples of human islets, treated with the harmine-LY364947 combination, immunolabeled for insulin- (green) and Ki67- (red), exemplifying unprecedented rates of proliferation. The white arrows illustrate beta cells labeled with Ki67; the red arrows indicate other non-beta cell types which are Ki67^{+}. The panels on the right are enlarged from the white box within the main figure. **C.** Examples of NKX6.1, insulin, Ki67 and a merged view illustrating co-immunolabeling of Ki67 and NKX6.1 in insulin^{+} cells. **D** and **E.** The effects of two other harmine analogues, INDY (IN) (Wang et al., 2015a) and leucettine-41 (Lu) (Tahtouh et al., 2012) on human beta cell labeling with Ki67 with or without addition of TGFβ inhibitors, LY and ALK5. **F. and G.** The effects of harmine and LY364947 alone or in combination on

human islets using BrdU (overnight exposure) and phospho-histone-3 (PHH3). Examples of photomicrographs are provided in Supplementary Figures 2C,D. Note that PHH3 captures only G2M phases of cell cycle, as compared to Ki67 and BrdU, which capture all phases of cell cycle, so that labeling indices for PHH3 are lower than for Ki67 and BrdU. **H.** Effect of the harmine-LY combination on adult human beta cell numbers as assessed by FACS counting using an internal recovery standard, Spherotech beads. **I.** Effects of the harmine-LY combination on numbers of Mel1-hESC-derived beta cells from four different batches of cells. Each pair of dots connected by a line represents one batch of hESC-derived beta cells. In all panels, drug treatments were for 96 hours, and all experiments were done on dispersed islets. In A and D-I, each black dot represents an individual human islet preparation. Numbers of donors and beta cells counted are provided in Supplemental Table 3. For all panels, [+]indicates $p < 0.05$ vs. control by paired T-test, and [§]indicates $p < 0.05$ by ANOVA. [++]indicates $p < 0.05$ vs. harmine treatment by paired T-test, and [§§]indicates $p < 0.05$ vs. harmine by ANOVA.
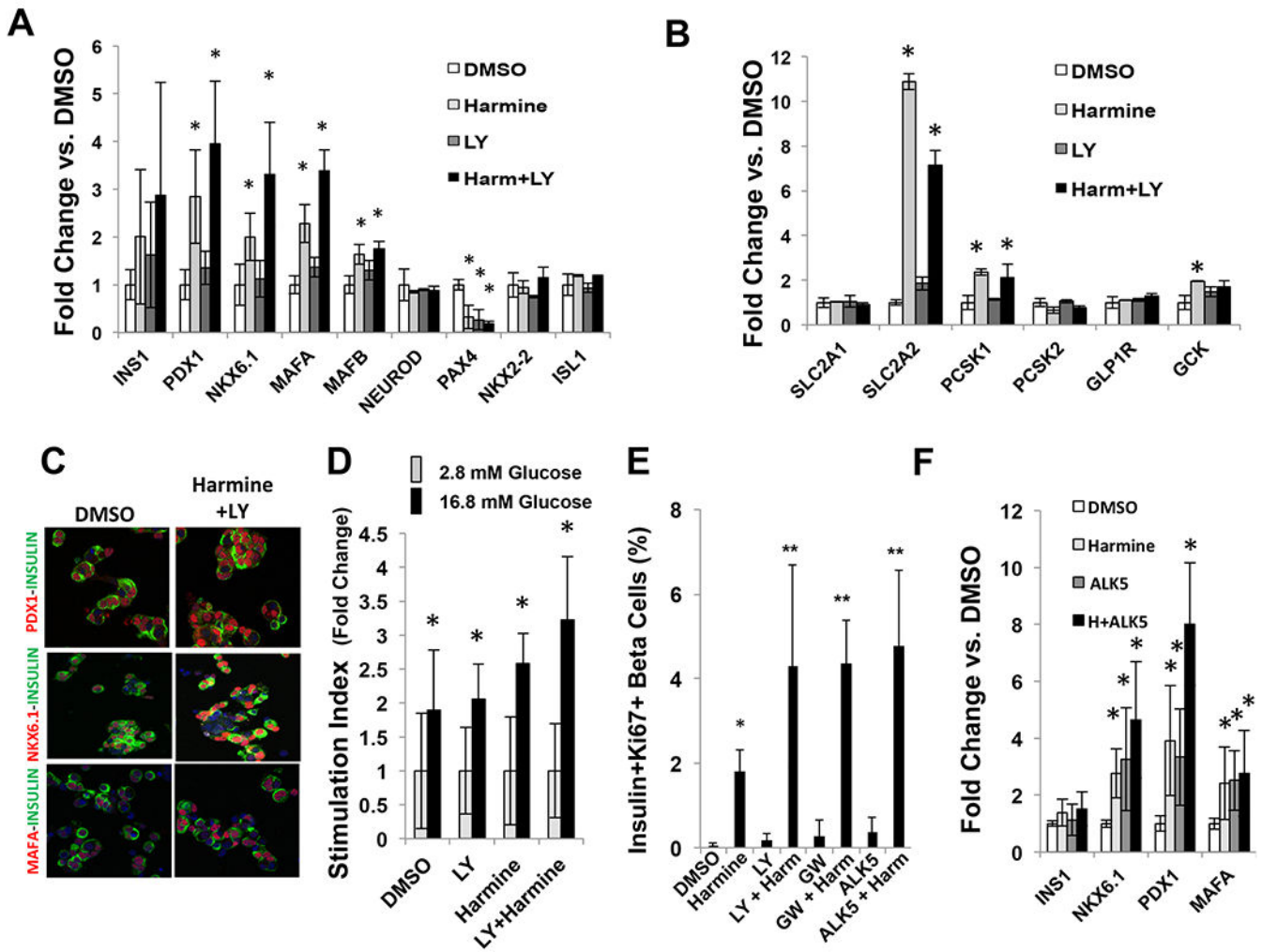
Figure 2. The harmine-TGFβSF inhibition combination increases beta cell differentiation markers in normal and T2D beta cells.

A,B. Effects of harmine and the harmine-LY364947 combination treatment for four days on key beta cell transcription factors and markers of beta cell differentiation in whole human islets assessed by qPCR. The panels include five human islet preparations. *indicates $p < 0.05$ vs. vehicle (DMSO) treatment. **C.** Immunocytochemistry on dispersed human beta cells (green) showing that combination treatment increases PDX1, NKX6.1 and MAFA (red) specifically in beta cells. Representative of experiments in three different human islet donor preparations. Brighter images are shown in Supplementary Figure 4A. **D.** Insulin secretion in response to low and high glucose in islets from eight different donors in the presence of vehicle, harmine, LY364947 or the harmine-LY364947 combination. *indicates $p < 0.05$ for high glucose vs. low glucose. **E.** Effects of harmine and TGFβ inhibitors on beta cell Ki67 immunolabeling in islets from six donors with T2D. *indicates $p < 0.05$ vs. control. **indicates $p < 0.05$ vs. harmine. **F.** Effects of harmine alone and with ALK5 on key beta cell transcription factors and markers in whole islets from six donors with Type 2 diabetes, as assessed by qPCR. Effects of additional TGFβ inhibitors on T2D islets are shown in Supplementary Figure 4B. *indicates $p < 0.05$ vs. control. All drug treatments were for 96

hours, and all experiments were performed on dispersed islets, except for panel D, which employed whole islets. Error bars in all panels indicate mean ± SEM. Numbers of donors and beta cells counted are provided in Supplemental Table 3.
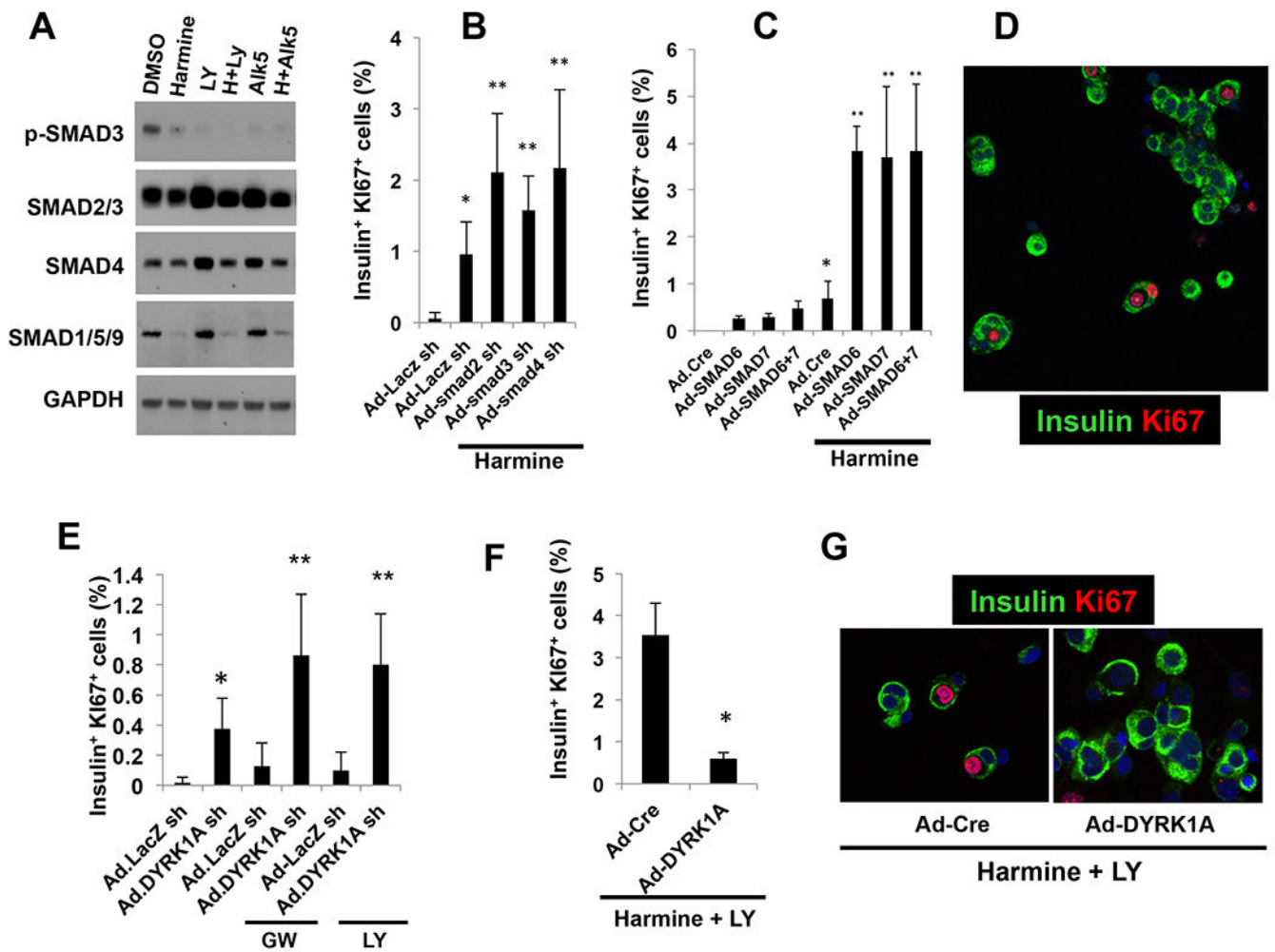
Figure 3. Requirements for DYRK1A and SMAD signaling.
A. Immunoblots of control, harmine-, LY364947-, ALK5 inhibitor- or combination-treated whole human islets. While SMAD2 and SMAD3 (detected by the same antibody) did not change, p-SMAD3 was reduced by harmine, and further reduced by LY364947 or ALK5 inhibitor and the combinations. SMAD1, 5 and 9 are also detected by a common antibody, and are reduced by harmine and the drug combinations. The immunoblots are representative of separate experiments in human islets from three different donors. **B.** Effects of a control adenovirus expressing an shRNA directed against LacZ and adenoviruses silencing SMAD2,3 and 4 (150 moi each) on Ki67 immunolabeling in harmine-treated human islets. **C.** Effects of adenoviral SMAD6 and SMAD7 overexpression (100 moi each) on beta cell proliferation, alone and in combination with harmine. **D.** An example of the mitogenic effects of SMAD7 silencing in human beta cells (green) on Ki67 immunolabeling. **E.** The effects of adenoviral silencing of DYRK1A in combination with TGFβSF inhibitors GW788388 or LY364947. Ad.shLacZ indicates a control sh-adenovirus for the Ad.shDYRK1A. **F.** Effect of adenoviral DYRK1A overexpression or a control adenovirus expressing Cre (Ad.Cre) on proliferation in human islets treated with the harmine-LY364947 combination. **G.** Examples of Ad.Cre- and Ad.DYRK1A-overexpressing viruses on Ki67

immunolabeling in human islets treated with harmine and LY364947. All adenovirus experiments were for 96 hours, and all experiments were done on dispersed islets. In all panels, error bars represent mean ± SEM, *indicates $p<0.05$ vs. control, and **indicates $p<0.05$ vs. harmine. Numbers of donors and beta cells counted are provided in Supplemental Table 3.
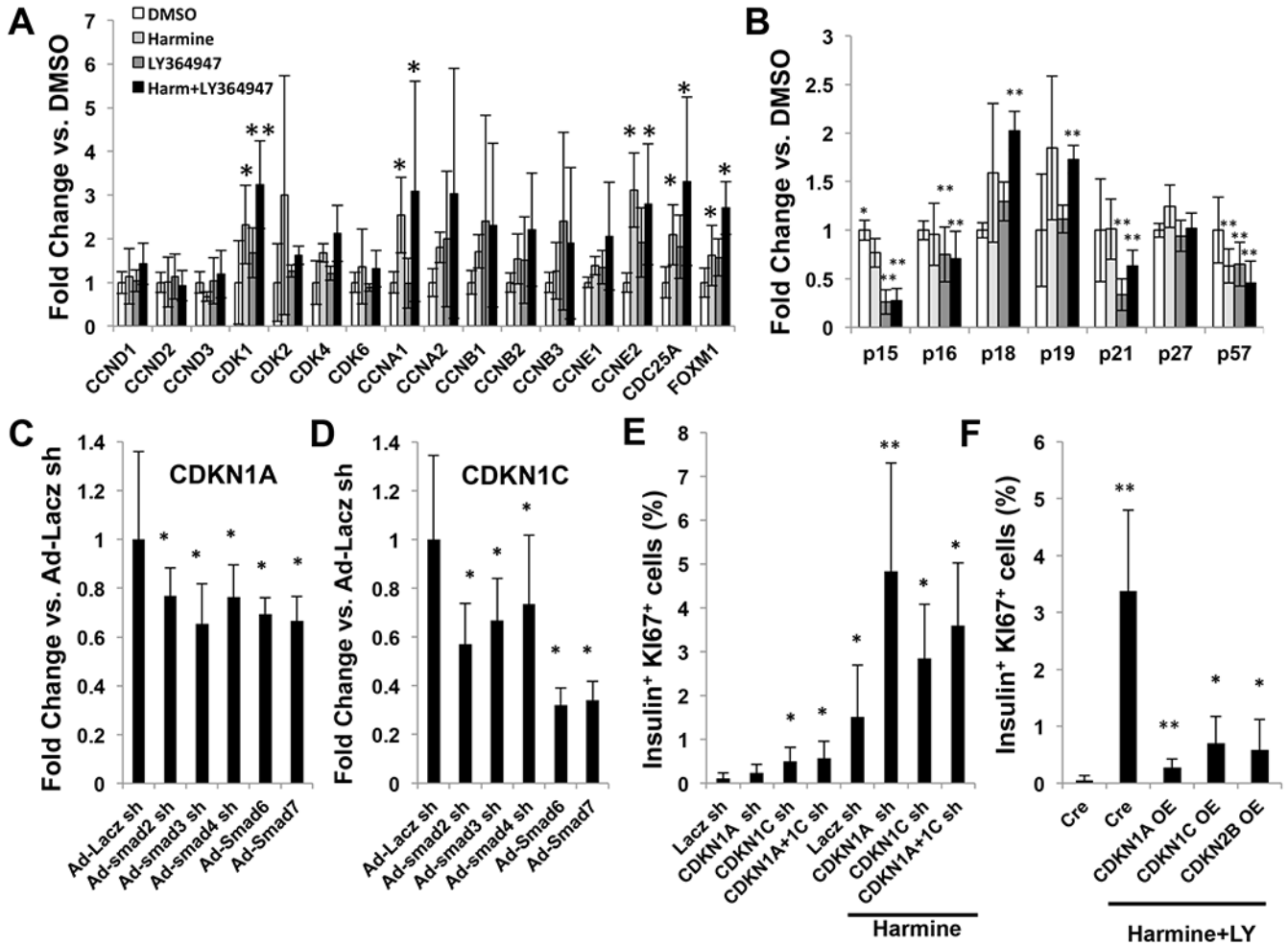
Figure 4. Changes in cell cycle molecule expression in response to harmine, LY364947, ALK5 inhibitor, and the combination.

A. The effects on vehicle (DMSO 0.1%), harmine (10 μM), LY364947 (5 μM), or the combination for 96 hours on gene expression in dispersed human islets for cell cycle activators, as assessed using qPCR. **B.** Comparable results for cell cycle inhibitors. **C,D.** The effect of silencing SMADs 2,3,4 or overexpressing SMADs 6 and/or 7 on expression of *CDKN1A* and *CDKN1C* in human islets as assessed using qPCR. **E.** The effects of silencing *CDKN1A, CDKN1C* and the combination on Ki67 immunolabeling in human beta cells in the presence or absence of harmine 10 uM. **F.** The effects of overexpression of *CDKN1A, CDKN1C* and *CDKN2B* in dispersed human islets for 96 hours on proliferation induced by the harmine- LY364947 combination. All experiments represent five human islet preparations, and error bars represent mean ± SEM. *indicates p.0.05 vs. control, and **indicates p<0.05 vs. harmine. Numbers of donors and beta cells counted are provided in Supplemental Table 3.
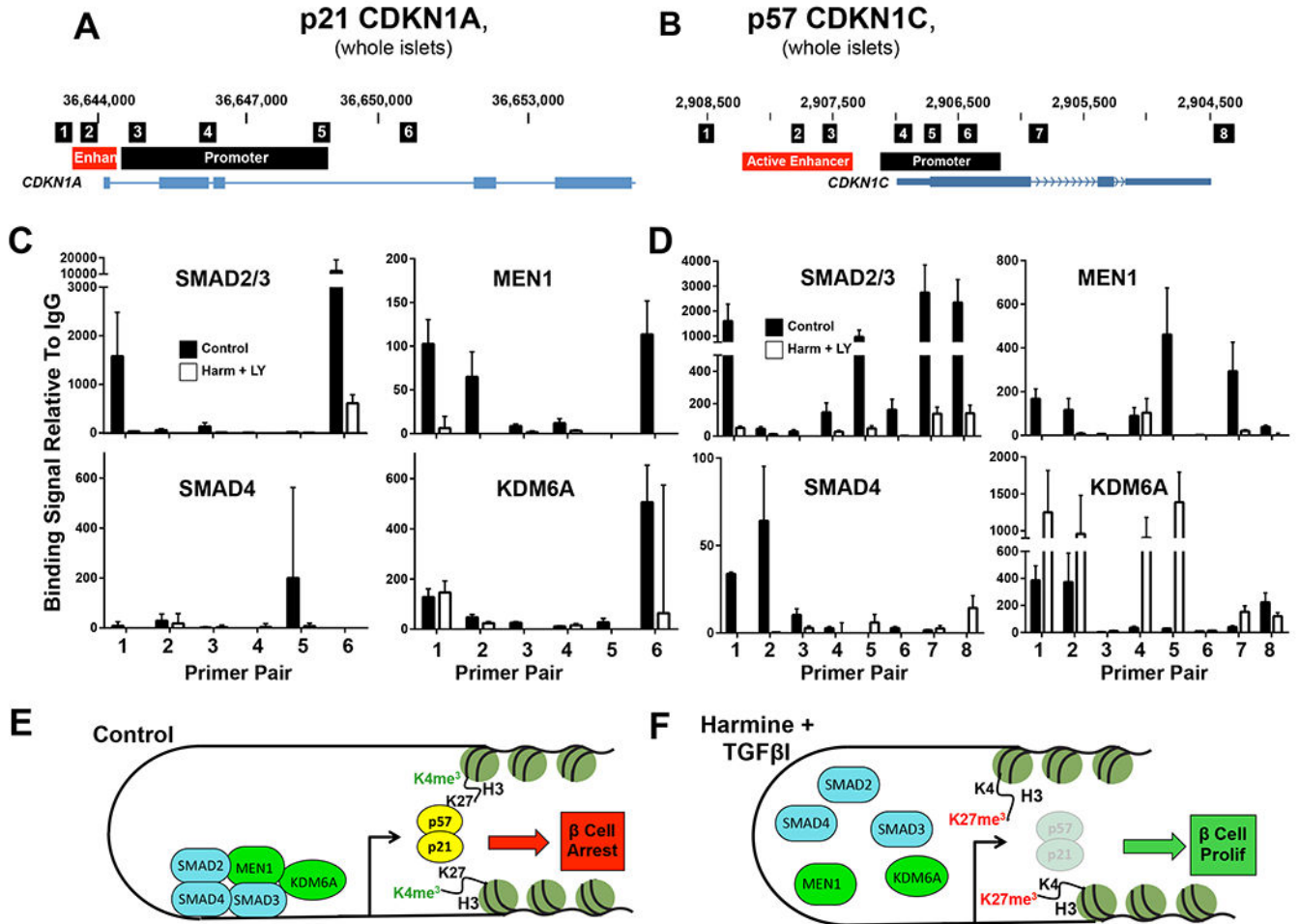
Figure 5. Direct interaction of SMADs and Trithorax members with the *CDKN1A* and *CDKN1C* loci in human islets.

A,B. Schematics of the human *CDKN1A* and *CDKN1C* loci from the hg19 UCSC genome browser, showing PCR products amplified in the primer pairs used for ChIP in the small black boxes, the gene bodies in blue below, and enhancers and promoters in orange and black respectively. Enhancer and promoter loci are derived from Pasquali and Ferrer (Pasquali et al., 2014). **C,D.** ChIP results in control (black bars) and harmine-LY364947-treated (white bars) human islets, with primer pairs corresponding to panels A and B along the x-axis. Primer pairs and locations for CDKN1A and CDKN1C are derived from (Koinuma et al., 2009; Pasquali et al., 2014; Yang et al., 2009). Experiments were performed on dispersed human islets. Drug treatment lasted for 96 hours. Error bars indicate SEM. Each experiment represents the mean of a minimum of three sets of human islets. **E,F.** Schematics indicating interactions of the SMADs and Trithorax members under basal conditions and following harmine-LY364947 treatment, respectively, illustrating that harmine-LY364947 treatment markedly alters SMAD-Trithorax binding to the *CDKN1A* and *CDKN1C* loci. Numbers of donors and beta cells counted are provided in Supplemental Table 3.
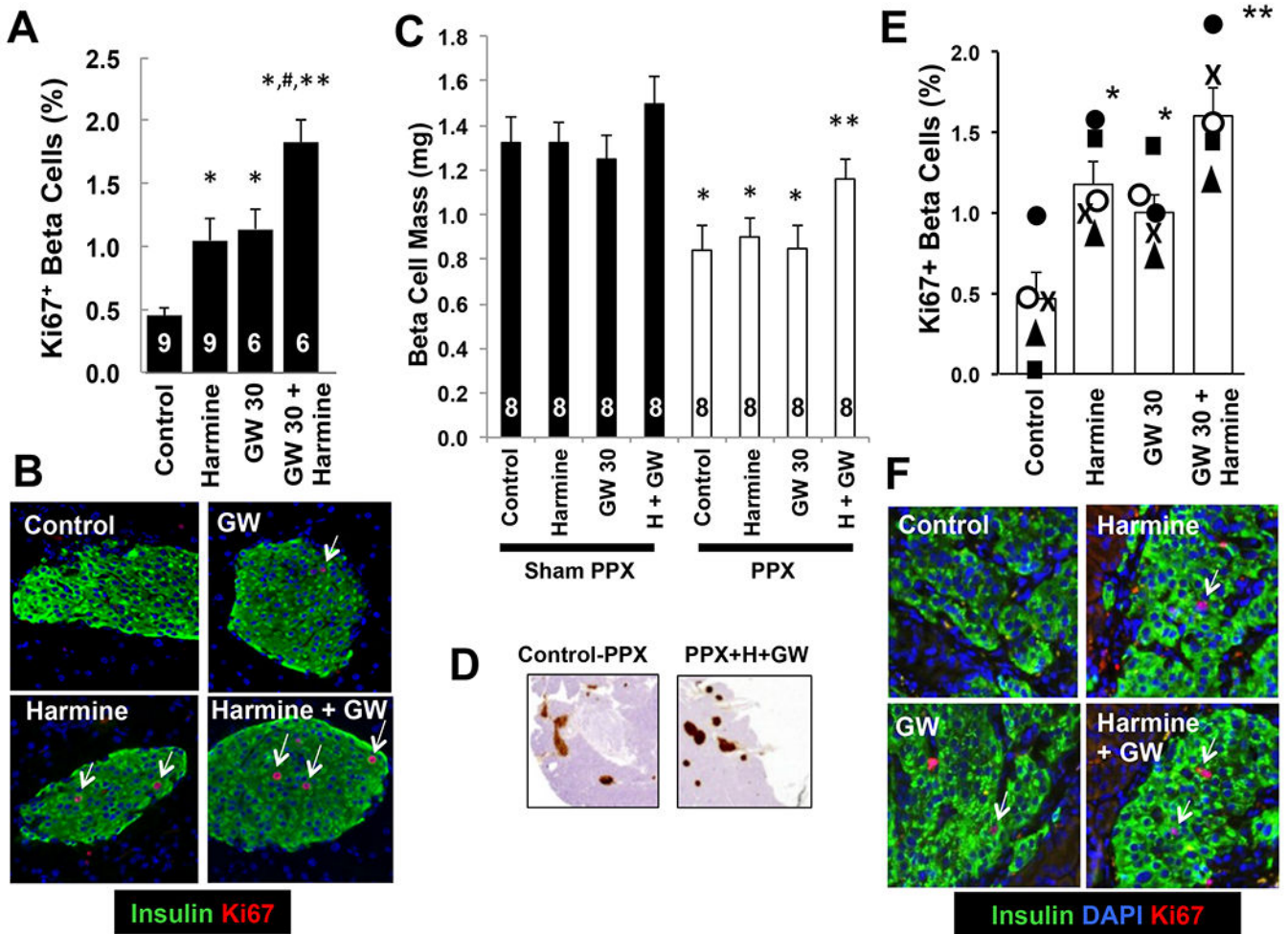
Figure 6. Effects of the harmine-TGFβ inhibitor combination in three *in vivo* models.
A. Intraperitoneal administration of saline (Control), harmine 10 mg/kg/day, GW788388 (GW) 30 mg/kg/day or the combination of harmine 10 mg/kg plus GW788388 30 mg/kg/d daily for seven days. After seven days of treatment, the pancreata were harvested and Ki67 and insulin immunolabeling quantified. The numbers of animals in each group are shown within the bars. A minimum of 2000 beta cells were counted for each bar shown. Error bars indicate SEM. *indicates $p < 0.05$ vs. control, # $p < 0.01$ vs. harmine or GW alone, and ** $p < 0.01$ vs. control, by one-way Bonferroni corrected ANOVA. **B.** Examples of Ki67 (red), DAPI (blue) and insulin (green) immunolabeling in each of the four groups in panel A. Arrows indicate examples of Ki67^{+} beta cells. **C.** The effects on total beta cell mass in eight groups of eight C57BL/6N mice receiving daily intraperitoneal vehicle (saline), harmine (10 mg/kg), GW788388 (30 mg/kg) or the harmine-GW788388 combination for seven days following sham or real 60% pancreatectomy (PPX). Error bars indicate SEM, *indicates $p < 0.05$ vs. sham PPX animals, and **indicates $p < 0.05$ vs. harmine or GW 30-treated PPX mice. **D.** Examples of pancreas remnants immunolabeled for insulin from mice undergoing PPX treated with control (saline) or the harmine-GW788388 combination. See Supplemental Figure 6 for details. **E.** The effects of control vehicle (saline), intraperitoneal harmine (10 mg/kg), GW788388 (30 mg/kg) or the harmine-GW788388 combination on human beta cell

proliferation for seven days in five sets of four NOD-SCID mice that received renal capsular islet transplants with 1000 human islet equivalents from five different islet donors, indicated by the squares, triangles, closed circles, open circles and "X" symbols. A minimum of 2000 beta cells were counted for each bar shown. Error bars indicate SEM *indicates $p < 0.05$ vs. control islets, and **indicates $p < 0.05$ vs. harmine and GW788388. **F.** Examples of Ki67 (red) and insulin (green) immunolabeling in human islets as in D. Arrows indicate examples of Ki67$^+$ beta cells.
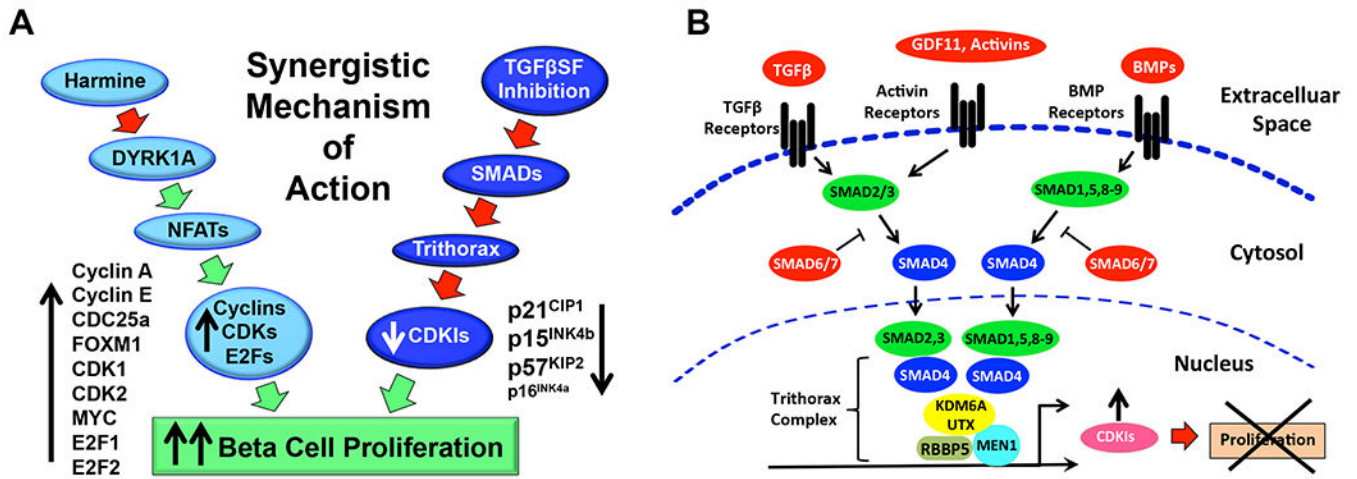
Figure 7. Models of TGFβ superfamily signaling and Harmine-TGFβ superfamily actions on human beta cell proliferation.

A. A simplified illustration of the synergistic mechanisms through which harmine and TGFβSF pathway inhibitors cooperate to enhance human beta cell proliferation. Harmine, acting on DYRK1A, primarily activates cyclins, cdks and related cell cycle activators. In parallel, TGFβSF pathway inhibitors relieve expression of cell cycle inhibitors, including *CDKN1A* encoding p21^{CIP}, *CDKN1C* encoding p57^{KIP}, and *CDKN2B* encoding p15^{INK4}. As suggested in Figure 3A, harmine also has direct or indirect effects on TGFβSF-SMAD signaling, and it is likely that DYRK1A has effects on other targets in addition to NFaTs. **B.** In the canonical TGFβ paradigm, ligands such as TGFβ, activins, inhibins, myostatin, GDF11, and bone morphogenic proteins (BMPs) bind to multi-subunit receptors that phosphorylate, and thereby activate, so-called receptor SMADs (SMADs 2,3, and 1,5,8/9). These are then able to heteromerize with SMAD4, a common SMAD, and the SMAD4 heteromers translocate to the nucleus where, among other things, they are incorporated into the chromatin-modifying and DNA-methylating Trithorax Complex, and thereby influence expression of multiple gene families. Adapted from Brown and Schneyer (Brown and Schneyer, 2010).